A palynological analysis of Late Cretaceous and Paleogene Strata from the Eclipse Trough, South Coast section, Bylot Island, Nunavut.

Jeremy Brittain

Partial Requirement for the Degree of Bachelor of Sciences, Honours
Department of Earth Sciences
Dalhousie University, Halifax, Nova Scotia, Canada
April 2016

Distribution License

DalSpace requires agreement to this non-exclusive distribution license before your item can appear on DalSpace.

NON-EXCLUSIVE DISTRIBUTION LICENSE

You (the author(s) or copyright owner) grant to Dalhousie University the non-exclusive right to reproduce and distribute your submission worldwide in any medium.

You agree that Dalhousie University may, without changing the content, reformat the submission for the purpose of preservation.

You also agree that Dalhousie University may keep more than one copy of this submission for purposes of security, back-up and preservation.

You agree that the submission is your original work, and that you have the right to grant the rights contained in this license. You also agree that your submission does not, to the best of your knowledge, infringe upon anyone's copyright.

If the submission contains material for which you do not hold copyright, you agree that you have obtained the unrestricted permission of the copyright owner to grant Dalhousie University the rights required by this license, and that such third-party owned material is clearly identified and acknowledged within the text or content of the submission.

If the submission is based upon work that has been sponsored or supported by an agency or organization other than Dalhousie University, you assert that you have fulfilled any right of review or other obligations required by such contract or agreement.

Dalhousie University will clearly identify your name(s) as the author(s) or owner(s) of the submission, and will not make any alteration to the content of the files that you have submitted.

If you have questions regarding this license please contact the repository manager at dalspace@dal.ca.

Grant the distribution license by signing and dating below.

Name of signatory

Date

Abstract

The South Coast section of Bylot Island contains Cretaceous and Paleogene outcrops making the island's strata integral in determining the geological history of eastern Arctic Canada. Biostratigraphy is the primary method to obtain ages of sedimentary rocks in the Labrador-Baffin Seaway. Dinocysts are key biostratigraphic markers because they evolve quickly, have a diverse morphology, and are widespread in marine sediments. Dinocysts have distinct tabulation that is used in taxonomy and nomenclature. Tabulation is the primary criteria used to identify dinocysts taxa. Analysis of palynological assemblages have determined new ages and paleoenvironments for Late Cretaceous to Early Paleogene strata at the South Coast section. The paleoenvironment of the South Coast section is neritic with distance from the coast increasing up section. One hiatus is present at the South Coast section. The Campanian section is missing where Early Maastrichtian strata unconformably overlie Coniacian to Santonian strata. Palynological assemblages have refined the Cretaceous-Paleogene boundary and place it in the base of the Pond Inlet formation. The taxa across the K/T boundary show little variation suggesting the regional dinocysts record does not show evidence of a major extinction event at the end of the Cretaceous.

Key Words: Bylot Island, palynology, dinocysts, biostratigraphy, Cretaceous, Paleogene, paleoenvironment

Table of Contents

Table of Figures

Table of Tables

Acknowledgements

I wish extend my gratitude to my supervisors Rob Fensome and Graham Williams for their time and effort towards this thesis; to the GSC Atlantic for allowing me to use their facilities and samples; to Elliot Burden, Kerry Sparkes, and James Waterfield for donating the samples to the GSC; and to Lawrence Plug for overseeing the Honours program at Dalhousie.

1.0 Introduction

Palynology is the study of organic walled microfossils. Fossilized pollen, spores, and dinoflagellate cysts (dinocysts) are collectively termed palynomorphs. Palynomorphs include key biostratigraphic markers that help determine ages of sedimentary rocks. Biostratigraphy is the primary method to obtain ages of sedimentary rocks because of the difficulty to obtain numerical ages in useful stratigraphic positions. Biostratigraphy is the only way to date strata in many of Canada's sedimentary basins. This thesis contains an in depth analysis of dinocyst assemblages from Late Cretaceous and Paleogene strata with the goal of refining age and paleoenvironmental interpretations of these strata and determining the position of the Cretaceous–Paleogene ("K/T") boundary.

In the eastern Arctic it is uncommon to find exposed Cretaceous and Paleogene rocks. The South Coast section of Bylot Island [Figure 1.1 and Figure 2.9] contains both Cretaceous and Paleogene outcrops, making the island's strata integral in determining the geological history of eastern Arctic Canada. Elliot Burden of Memorial University and two students, Kerry Sparkes and James Waterfield, collected samples from the South Coast section for graduate studies. Sparkes' thesis (1989) used palynological analysis of terrestrial palynomorphs to determine the ages and depositional environments of the Eclipse Trough strata. Waterfield (1989) completed a similar palynological analysis, as well as an extensive sedimentological study of Eclipse Trough. Sparkes (1989) and Waterfield (1989) did not examine the dinocysts in detail, focusing on spores and pollen (miospores). Dinocysts are more useful biostratigraphic markers than miospores because they evolve quickly, have a diverse morphology, and are widespread in marine sediments. However, ages and paleoenvironments are best determined considering dinoflagellates and miospores together. The Memorial group donated their remaining unprocessed samples to the Geologic Survey of Canada (Atlantic).

The Geological Survey of Canada (GSC) launched the Geo-Mapping for Energy and Minerals (GEM) program in 2008 [NRGC 2016]. The five-year, $100 million program was designed to improve the geological understanding of, and facilitate resource development in, Canada's North. The GEM program produced over 700 maps and reports [NRGC 2016]. The success of this program resulted in a seven-year, $100 million program renewal in August of 2013 [NRGC 2016]. The results from the GEM program are expected to create more than $500 million in economic activity over the next 10-15 years [NRGC 2016].

For over a decade, and latterly as part of the GEM program, GSC Atlantic (GSCA) has been conducting a joint palynological study with the Geological Survey of Denmark and Greenland (GEUS). This study focuses on the Labrador Sea, Davis Strait, and Baffin Bay (collectively the Labrador-Baffin Seaway). The Labrador-Baffin Seaway separates Canada and Greenland. The goal of this joint study is to fill existing gaps in the biostratigraphic record using dinoflagellates and miospores, as well as refine stratigraphic correlation between the Canadian and Greenland margins. Samples used in the joint GSCA-GEUS study are mostly cuttings from offshore exploration wells. Cuttings samples tend to be widely spaced and prone to contamination. So related surface sections, like those on Bylot Island, are key to a full understanding of the regional stratigraphy. Bylot Island has the most complete Late Cretaceous-Paleocene onshore surface sections close to the Canadian margin of the Labrador-Baffin Seaway. Samples for this thesis are from the South Coast section in the Eclipse Trough of Bylot Island, Nunavut, Canada [Figure 1.1 and Figure 2.9]. Ages and paleoenvironments determined in this thesis will help fill existing gaps in the biostratigraphic and paleoenvironmental records, helping to refine the current understanding of the Labrador-Baffin Seaway.

Figure 1.1 - Map showing Bylot Island, Nunavut [Adapted from Google Earth]

2.0 Background information

2.10 Dinoflagellates and their cyst morphology

Dinoflagellates constitute the phylum Dinoflagellata. To be included in this phylum, an organism must have a life-cycle in which the cell is motile with two flagella and/or contain a specific type of nucleus termed a dinokaryon [Fensome et al. 1993]. The dinokaryon is a nucleus that lacks histones and, unusually for eukaryotes, the chromosomes remain condensed between episodes of cell division. Dinoflagellates are single-celled protists that range in size from five µm to two mm in diameter, but are typically between 20 and 200 µm. Dinoflagellates exist today mostly as planktonic organisms living in oceans, seas, and freshwater lakes. The cysts (dinocysts) of some lineages are found in the fossil record. The oldest fossilized dinocysts are from the Middle Triassic [Riding et al. 2010]. Approximately 50% of dinoflagellates are autotrophic (meaning that they photosynthesize), while the other 50% are parasites, heterotrophs, or saprophytes [Fensome et al. 1996]. Dinoflagellates can have complex life cycles with multiple stages, but most have a motile stage and some a cyst stage. During the motile stage a dinoflagellate has two flagella that act to propel the cell through the water. The transverse flagellum lies in the cingulum [Figure 2.1], which is a groove that wraps around the equator of the organism [Fensome et al. 1996]. The longitudinal flagellum is located in the sulcus and trails from the cingulum posteriorly [Figure 2.1] [Fensome et al. 1996]. Together, the two flagella, propel the organism forwards with a spiralling motion.

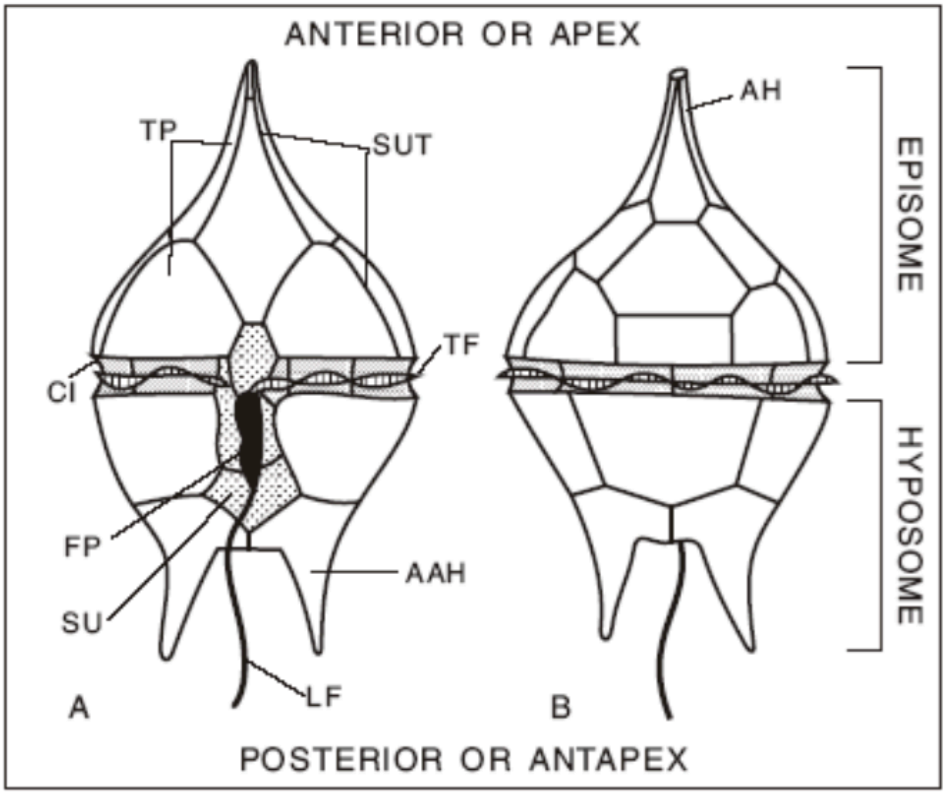

Figure 2.1 - Important morphological features. **A)** Ventral surface **B)** Dorsal surface. **TP** = thecal plates, **SUT** = sutures, **AH** = apical horn, **CI** = cingulum, **TF** = transverse flagellum, **LF** = longitudinal flagellum, **SU** = sulcus, **FP** = flagellar pore. [from Williams et al. 2009]

A cell membrane typically binds dinoflagellate cells [Fensome et al. 1993]. Below the cell membrane is a single layer of vesicles that, in some cases, contain cellulosic plates (thecal plates) [Figure 2.1]. Tabulation [Figure 2.2] refers to the structure and orientation of these thecal plates and is the most valuable criteria in dinocyst taxonomy and nomenclature. It is important to note that fossilized dinocysts have only reflections of thecal plates, not the original plates [Fensome et al. 1993]. There are three common types of cyst, resting cysts, short-term temporary cysts, or vegetative cysts. Bacteria will quickly destroy vegetative and short-term cysts, while resting cysts are generally more resistant and have a greater chance of preservation [Fensome et al. 1996]. The resistant organic material composing the wall of many resting cysts is known as dinosporin and is a complex organic polymer specific to dinoflagellates [Fensome et al. 1996]. Alternatively, calcium carbonate or rarely silica may compose the wall of resting cysts [Fensome et al. 1996], though such cysts are not preserved in palynological assemblages. When an organism transitions from the dormant cyst stage to motile stage it will excyst through an aperture that commonly corresponds to one or more thecal plates [Figure 2.4]. The empty cyst falls to the sea floor, where it may be preserved [Fensome et al. 1996]. The excystment opening is called the archeopyle and its cover, which becomes partially or wholly detached, is called the operculum [Fensome et al. 1996]. Evitt (1961) coined the term archeopyle for the opening in a fossil dinoflagellate formed by the release of a single or group of plates, thus demonstrating that fossil dinoflagellates are cysts.

Most fossil dinoflagellates have one of two types of tabulation: gonyaulacoid and peridinioid. Tabulation varies among gonyaulacoids and peridinioids, but in both types the thecal plates are arranged in several latitudinal series and a longitudinal sulcal series [Williams et al. 2009] [Figure 2.2]. The latitudinal series relate to the apex, cingulum, and the antapex of the body [Figure 2.1]. Each latitudinal series is expressed according to Kofoid's alphanumeric system (e.g., 1" for the first precingular plate) [Fensome et al. 1993] [Figure 2.2]. Numbering of the plates within each latitudinal series begins midventrally with the first plate in line with, or left of, the sulcus. Plates contacting the apex are apical plates and are denoted by (‘). The plate series immediately above (anterior to) the cingulum are precingular plates (“). The series immediately below (posterior to) the cingulum are postcingular plates (“‘). Plates contacting the antapex are antapical plates (““).

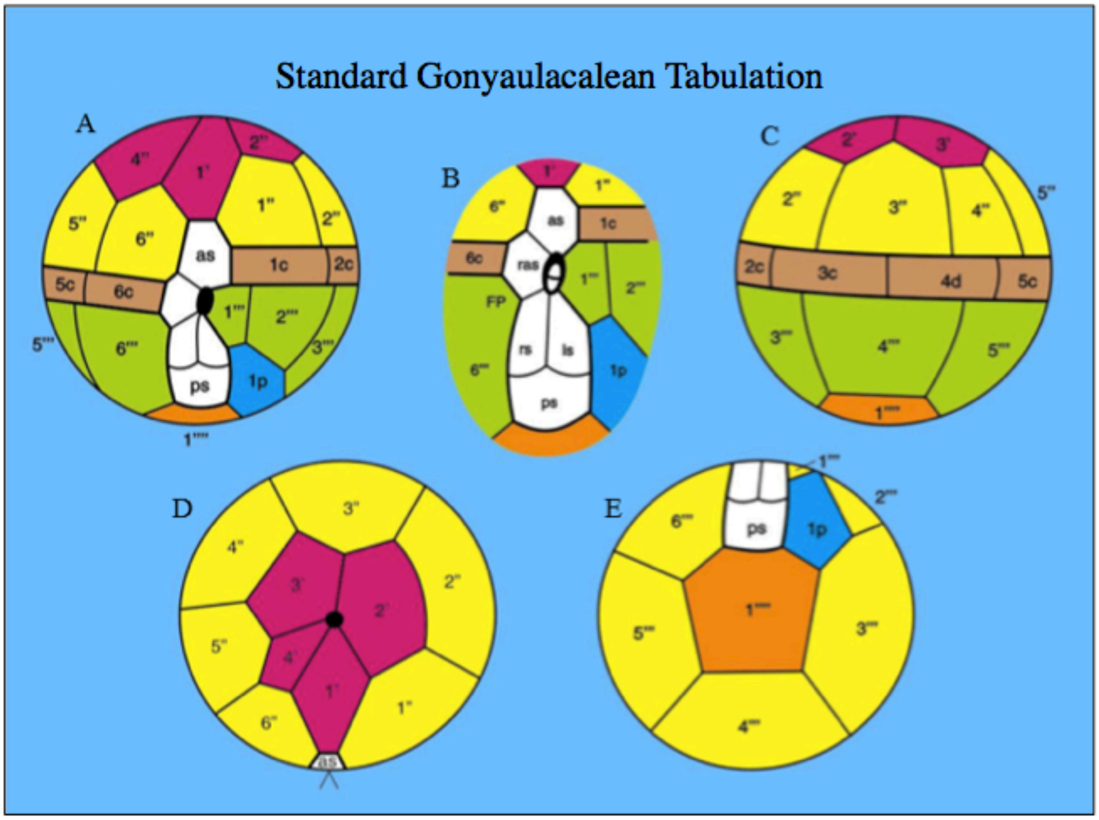

Figure 2.2 - Standard Gonyaulacalean tabulation. **A)** ventral view **B)** sulcal view **C)** dorsal view **D)** apical view **E)** antapical view. **Pink** = apical plates (‘), **Yellow** = precingular plates (“), **Tan** = cingular plates (c), **Green** = postcingular plates (“‘), **Orange** = antapical plate (““), **White** = sulcal plates (s). [Credit to R.A. Fensome, unpublished course graphic]

Gonyaulacoids [Figure 2.2] typically have four apical plates, six precingular plates, five or six cingular plates, six postcingular plates, and one antapical plate [Williams et al. 2009]. A single posterior intercalary plate (1p) is unique to gonyaulacoids [Figure 2.2 blue]. Peridinioids [Figure 2.3] typically have four apical plates, seven precingular plates, four to six cingular plates, five postcingular plates, and two antapical plates. Peridinioids have three distinct anterior intercalary plates on the dorsal side of the body [Figure 2.3]. These three plates are located between the apical and precingular plates on the dorsal surface. Posterior intercalary plates are present in some genera with peridinioid.

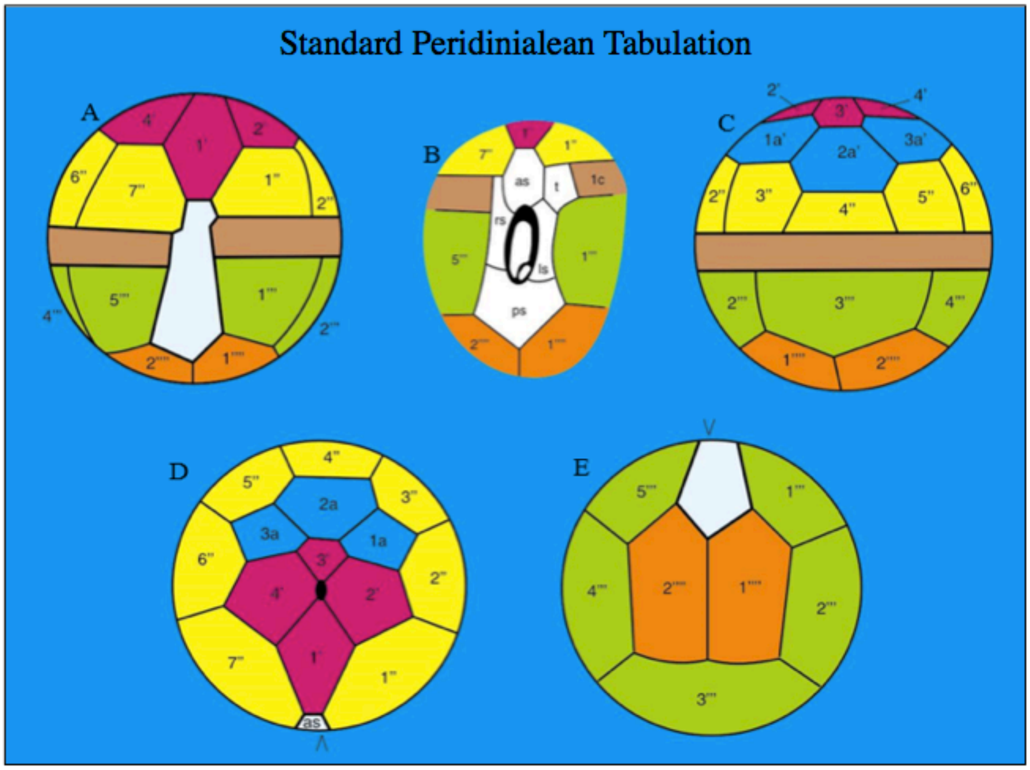

Figure 2.3 - Standard Peridinialean tabulation. **A)** ventral view **B)** sulcal view **C)** dorsal view **D)** apical view **E)** antapical view. **Pink** = apical plates (‘), **Yellow** = Precingular plates (“), **Blue** = Intercalary plates (a), **Tan** = Cingular plates (c), **Green** = Postcingular plates (“‘), **Orange** = Antapical plates (““), **White** = Sulcal plates (s). [Credit to R.A. Fensome, unpublished course graphic]

Evitt (1961) realized that the form (shape and plates involved) of the archeopyle and operculum are critical because they are usually the only preserved indication of tabulation. The three main archeopyle forms are apical, precingular, and intercalary. An apical archeopyle (A) forms when the entire apical latitudinal series is lost [Figure 2.4B]. A precingular archeopyle (P) forms when one or more precingular plates are lost [Figure 2.4E]. An intercalary archeopyle (I) forms when a dinocyst loses one or more mid-dorsal anterior intercalary plates [Figure 2.4B].

Figure 2.5 shows the form variations that can occur in dinocysts with simple (I_{2a}) intercalary archeopyles. Intercalary archeopyles involving more than one intercalary plate will have more variation than simple (I_{2a}) intercalary archeopyles [Figure 2.5]. These multiplate archeopyles will give a better indication of tabulation. Determining the archeopyle is critical because it may be the only tabulation indicator present.

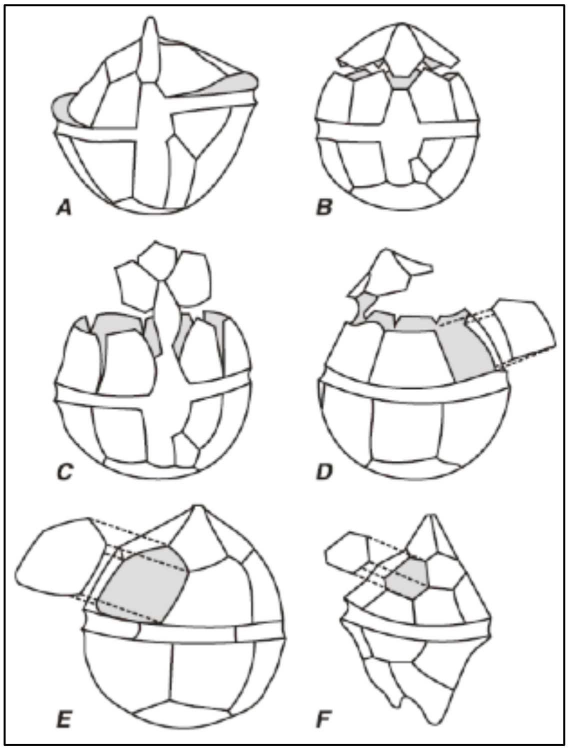

Figure 2.4 - Types of excystment archeopyles. **A)** Epitractal archeopyle with operculum adnate ventrally. **B)** Simple apical archeopyle. **C)** Apical Archeopyle (adnate) with accessory excystment sutures between precingular plates. **D)** Apical Archeopyle (adnate) with accessory precingular. **E)** Simple precingular archeopyle. **F)** Simple intercalary archeopyle. [from Williams et al. 2009]

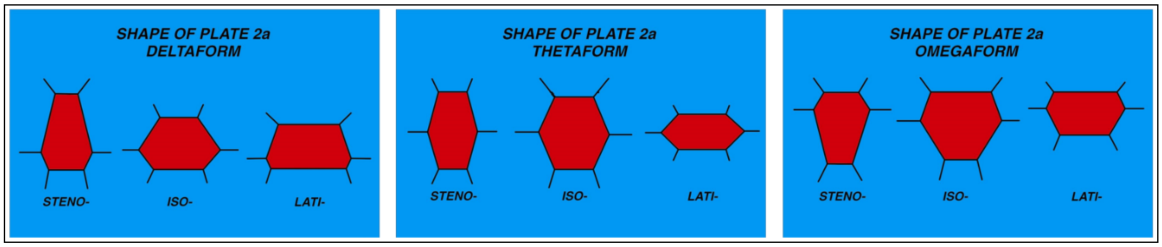

Figure 2.5 - Variations of simple (I_{2a}) hexa intercalary archeopyles. [Credit to R.A. Fensome, unpublished course graphic, after Bujak and Davies 1983]

The presence of spines or processes is another taxonomically valuable morphological feature. Proximate cysts [Figure 2.6 A] have no processes or spines, while chorate cysts [Figure 2.6 B] by definition, have well-developed processes or spines radiating from the central body [Williams et al. 2009]. Cysts containing processes that are less than 30% of their central body diameter are termed proximochorate [Figure 2.6 C].

Dinocysts are typically constructed of two walls, an inner wall (endophragm) and an outer wall (periphragm). Cavate cysts have two or more walls that are not in continuous contact [Williams et al. 2009]. In cavate cysts the endophragm forms an inner body (endocyst) and the periphragm forms an outer body (pericyst). The endocyst and pericyst will have corresponding archeopyles termed the endoarcheopyle and periarcheopyle; the endoarcheopyle and periarcheopyle are generally but not always identical in plate composition. Acavate cysts have a single wall layer termed the autophragm. It is important to note that terms such as proximate, chorate, and cavate are merely descriptive terms and generally do not specifically indicate taxonomic relations. However, understanding the nature of processes was emphasized in this thesis and helped distinguish between genera with similar or identical tabulation.

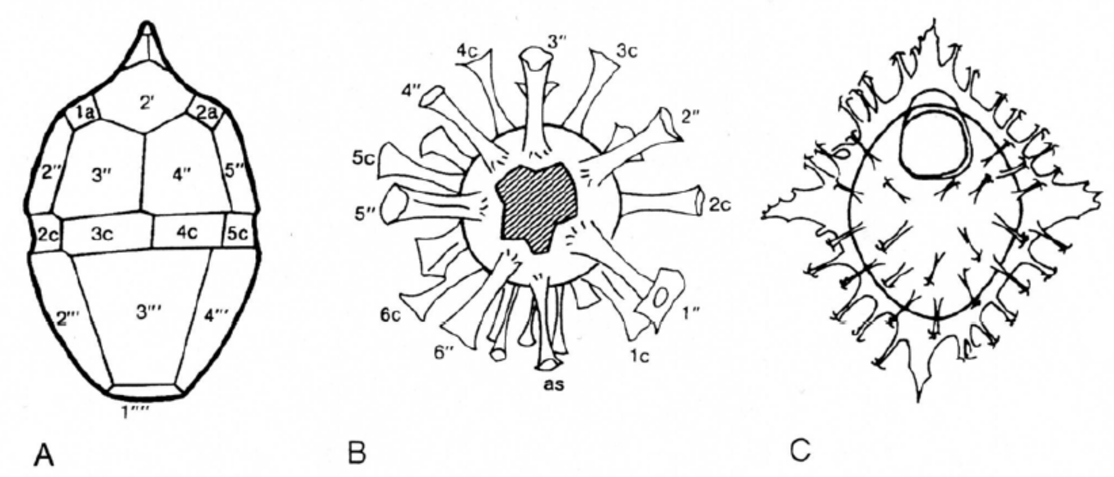

Figure 2.6 – Examples of proximate cyst (**A**), chorate cyst (**B**), and proximochorate cyst (**C**).
[from Williams et al. 2009]

2.11 Miospores

The collective term miospores includes all pollen and small spores and excludes megaspores. Some lower plants (e.g., ferns) have spores, which may all be of the same size (homospores) or of two sizes, smaller (male) microspores and larger (female) megaspores [Falcon-Lang et al. 2014]. Spores only germinate in water because earth's first plants grew in moist environments [Falcon-Lang et al. 2014]. Eventually microspores evolved into pollen grains that could be transported by wind. In the Late Devonian, some plants retained their megaspores with the prospect that windblown microspores/pollen would fertilize them; megaspores thus fertilized and became seeds [Falcon-Lang et al. 2014]. Seeds are more capable of withstanding dry and harsh climates allowing land plants to expand their range. Conifers and ferns dominated during the Late Cretaceous and Paleocene [Falcon et al. 2014]. Angiosperms were present during this time, but they did not dominate until the Oligocene [Falcon-Lang et al. 2014].

Bisaccate grains are the pollen of coniferous trees. Bisaccate pollen have two 'bladders' attached to the central body that fill with air and allow for the grains to travel long distances in the air. Wind and other agents have the ability to transport miospores from terrestrial environments to marine environments where they may sink to the seafloor. This is how terrestrial miospores and marine dinocysts are found in the same strata and palynomorph assemblages. The proportions of miospores to dinocysts can be an important indicator of depositional environment. Miospores tend to be more abundant in marine sediments that are closer to land than in offshore sediments.

2.20 Biostratigraphy and paleoenvironments

Biostratigraphic and paleoenvironmental results are typically based on analysis of palynological assemblages, lithostratigraphy, and well logs. The concepts of first and last occurrences are critical for biostratigraphy. First occurrence (FO) is the lowest or oldest occurrence of a taxon in a surface section or well. Last occurrence (LO) is the highest or youngest occurrence of a taxon in a surface section or well; LOs and FOs can be thought of as extinctions and originations of a taxon, respectively.

Miospores offer information on terrestrial paleoenvironments whereas dinocysts offer information on aquatic, mostly marine, paleoenvironments. Counts of dinocysts and miospores in the unsieved slide (see chapter 3.1) are made for quantitative analysis and give a general indication of distance from the coastline. However, this information can be misleading because bisaccate pollen (a terrestrial miospore) have the ability to be transported long distances resulting in an abundance of bisaccates in offshore samples.

Dinocysts are especially informative as they yield information from freshwater environments to open oceans. But there are caveats: since dinoflagellates are planktonic organisms they are not as reliable of a water depth indicator as benthic foraminifera. However, this limitation is overcome by the paleoenvironmental preferences shown by certain genera [Figure 6.2]. Consequently, individual dinocysts can be restricted to (or especially abundant) in non-marine, lagoonal, coastal, inshore, or offshore settings and will give useful clues to the paleoenvironment.

2.30 Tectonic History of the Labrador-Baffin Seaway

In the latest Cretaceous, Greenland began to separate from the eastern margin of Arctic Canada, forming the Labrador-Baffin Seaway [Monger et al. 2014]. Sea-floor spreading began 62-56 Ma and separated Greenland and Eurasia from the North American plate. During sea-floor spreading Greenland rotated counter-clockwise away from North America, effectively widening the seaway [Monger et al. 2014]. Rifting between Greenland and Eurasia began while sea-floor spreading was widening the Labrador-Baffin Seaway, effectively establishing Greenland as distinct tectonic plate. Sea-floor spreading in the Labrador-Baffin Seaway stopped in the Latest Eocene (approximately 34 Ma) and Greenland once again became part of the North American plate [Monger et al. 2014]. Sea-floor spreading still occurs between the North American plate (including Greenland) and the Eurasian plate, as the Norwegian Sea widens.

A rifting phase in the Early Cretaceous (approximately 100 Ma) developed a series of rift basins in the Labrador-Baffin Seaway and along its margins [Nøhr-Hansen et al. in press]. These rift basins are of significant hydrocarbon interest [McGregor et al. 2014] [Nøhr-Hansen et al. in press]. Uplift from lithospheric upwelling caused sedimentation to increase prior to sea-floor spreading [Monger et al. 2014]. Outpouring of basalt in west-central Greenland and southeast Baffin Island [Figure 2.7] from the Late Danian to the Thanetian (62-56 Ma) marks the transition from a rifting to a drifting phase [Nøhr-Hansen et al. in press]. Sea-floor spreading continued widening the Labrador-Baffin Seaway and ultimately put Greenland on a collision course with Arctic Canada. The result was the Eurekan Orogeny, a late Eocene fold-and-thrust belt on Ellesmere and neighbouring islands [Oakey et al 2012]. The change from drift to post-drift occurred post collision and saw large volumes of Late Cretaceous and Cenozoic sediment erode from the surrounding landmasses and become deposited in the sedimentary basins.

Plate tectonics is a primary driver in changing environments. It can cause changes in latitude, moving regions into new climatic zones. Rising or falling sea level may impact terrestrial and marine life. Sedimentation rates increase as accommodation space is created. All of these changes may be reflected in varying palynological assemblages that are found throughout the Labrador-Baffin Seaway strata and on its margins, for example the Bylot Island strata.

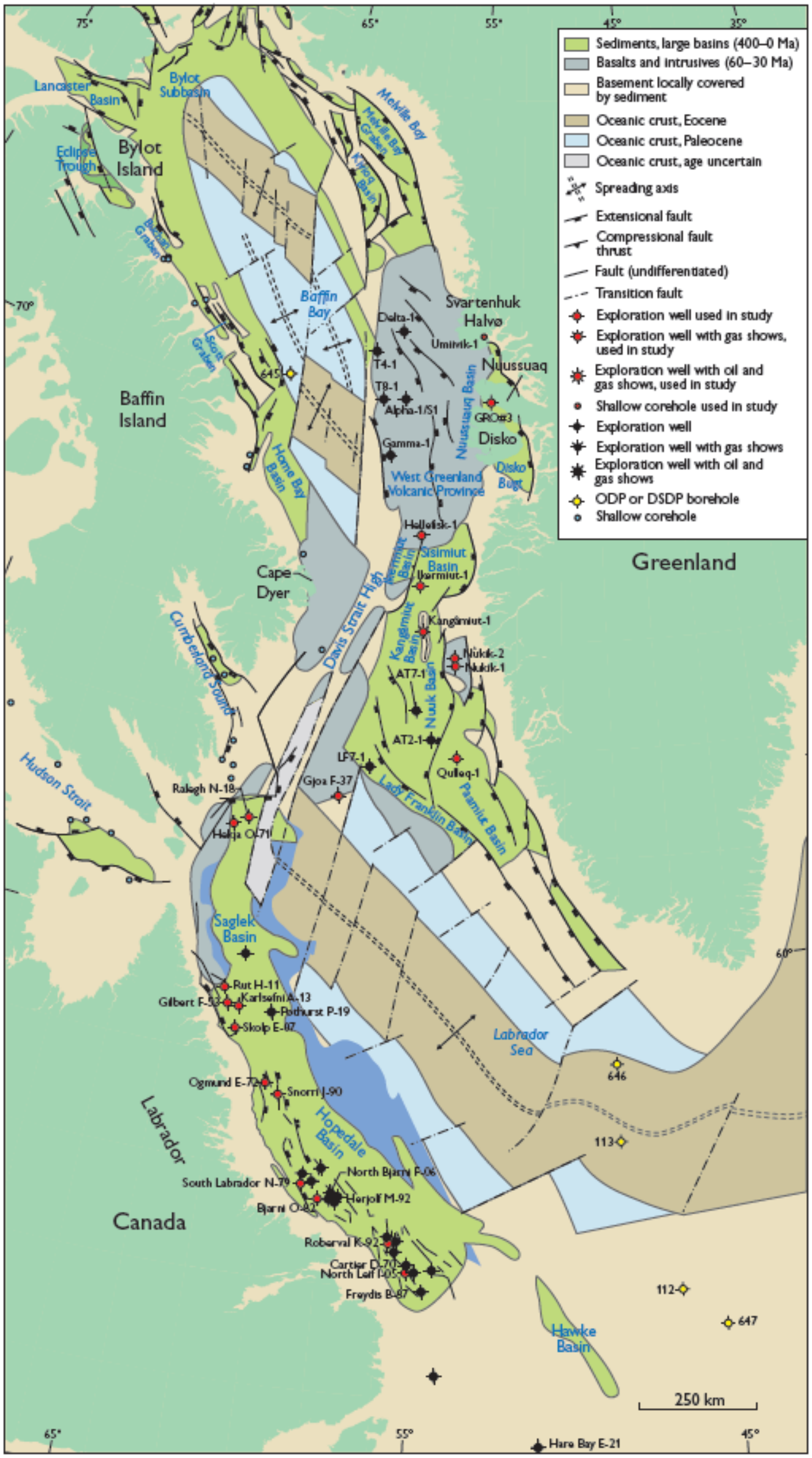

Figure 2.7 – Tectonic structures associated with the formation of the Labrador Baffin Seaway. [from Nøhr-Hansen et al. in press]

2.40 Bylot Island Geology

Bylot Island is an 11,000 km^2 landmass located along the eastern Canadian margin of the Labrador-Baffin Seaway [Figure 2.8]. Archean and Paleoproterozoic rocks comprise the Byam Martin Mountain Range [Figure 2.8][Figure 2.9] that runs east to west across Bylot Island [Williams 2013]. The Byam Martin Mountain range separates the North Bylot Trough and the southern Eclipse Trough [Figure 2.9].

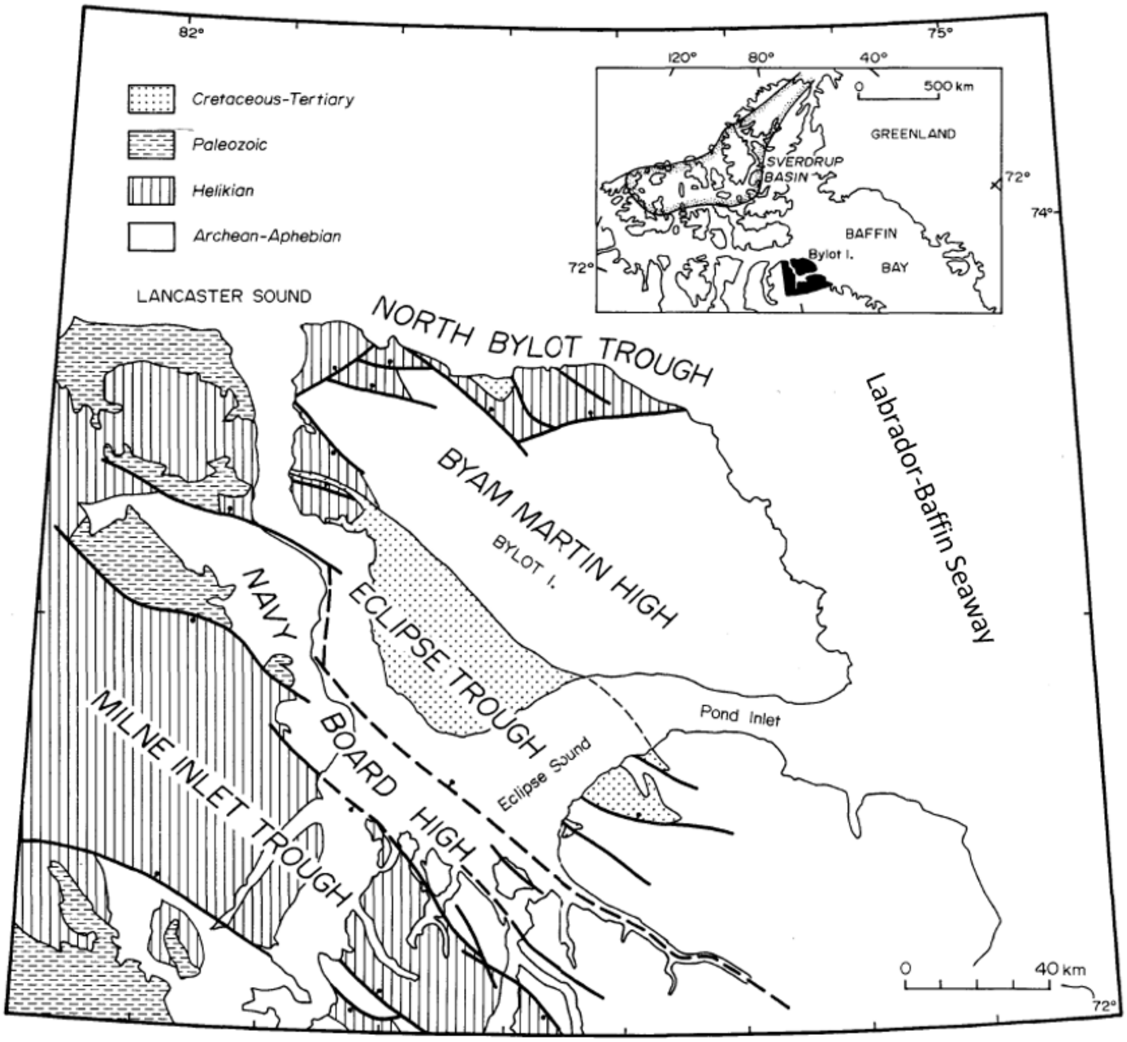

Figure 2.8 - Basic geological map of Bylot Island. [adapted from Miall et al. 1980]

The samples used for this thesis are from South Coast section outcrops in Eclipse Trough [Figure 2.9]. Eclipse Trough is a graben structure that is a part of the North Baffin Rift Zone, a series of horst and graben structures with a Precambrian basement [Jackson et al. 1975] [Harrison et al. 2011]. The Eclipse Trough is a northwest plunging, fault-bounded, basin that contains Cretaceous to Paleogene rocks [Harrison et al. 2011]. The outcrop area extends approximately 150 km in a northwest-southeast direction and comprises Cretaceous-Paleogene succession approximately 3320 m thick [Harrison et al. 2011]. Glacial deposits dominate Quaternary geology on Bylot Island. These glacial deposits stem from local mountain glaciers in the Byam Martin Range, as well as from the Laurentide Ice Sheet [Klassen 1993].

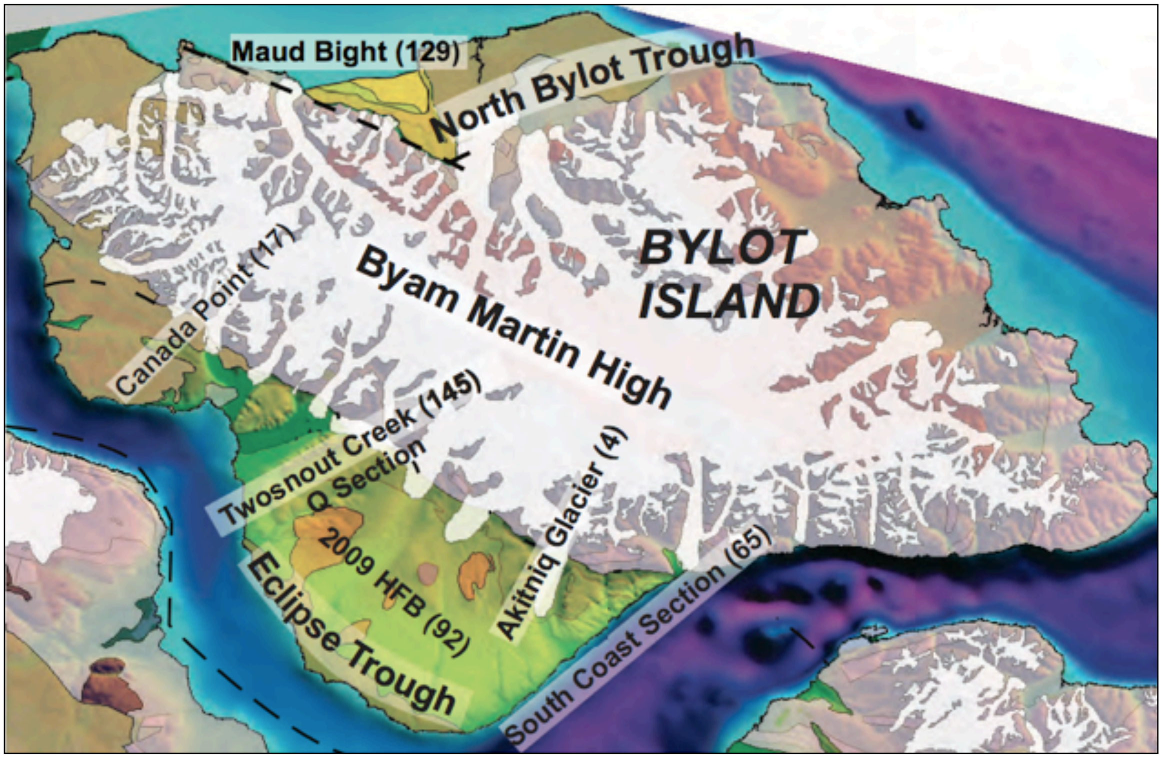

Figure 2.9 - Map of Bylot Island showing important sections. [Map provided by Lisel Curry, GSC Calgary]

2.50 Eclipse Trough Stratigraphy

Miall et al. (1980) distinguished three formations in what they called the Eclipse Group. The lowermost unit is the Hassel Formation, which is unconformably overlain by the Kanguk Formation. The uppermost unit is the Eureka Formation. Stratigraphy is presented in Table 2.50.

Table 2.1 - Stratigraphy of Eclipse Trough [adapted from Miall et al. (1980), Sparkes (1989), and Waterfield (1989)]
(U: Upper, L: Lower)

Age	Formation	Member [Miall et al. 1980]	formation [Sparkes 1989] [Waterfield 1989]	Lithology
Upper Palaeocene to Lower Eocene	Eureka Sound	U mudstone	-	Mudstone, minor sandstone
		U sandstone	Pond Inlet (at Twosnout)	Immature sandstone, minor siltstone, mudstone
		L mudstone	Bylot Island Navy Board	Mudstone, minor sandstone
		L sandstone	Pond Inlet (at South Coast)	Glauconitic sandstone
		Unconformity		
Campanian to Maastrichtian	Kanguk	Sandstone	Sermilik	Immature sandstone, minor siltstone, mudstone
		Mudstone	Byam Martin	Mudstone
		Unconformity		
Albian To Cenomanian	Hassel	-	-	Sandstone, minor mudstone

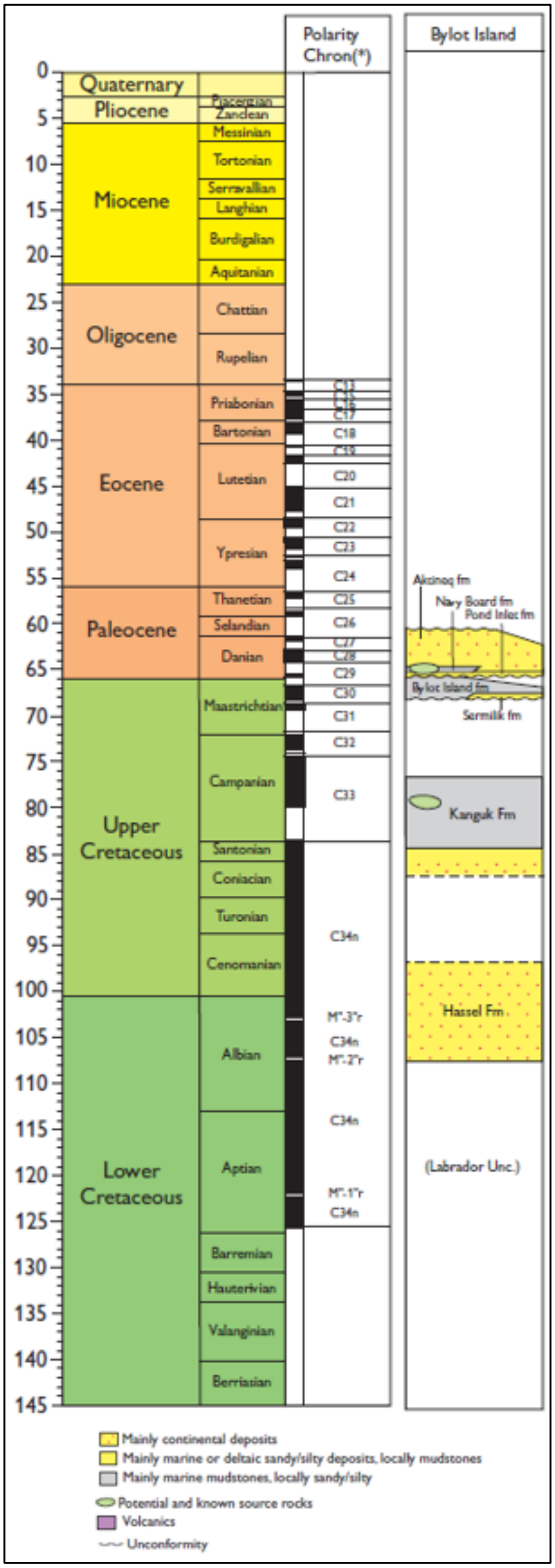

Figure 2.10 - Stratigraphic log of formations in Bylot Island's Eclipse Trough. [from Nøhr-Hansen et al. in press]

2.51 Hassel Formation

The Hassel Formation unconformably overlies Precambrian basement rocks and marks the base of sediment infill in Eclipse Trough [Miall 1980]. The thickness of the Hassel Formation is highly variable throughout Eclipse Trough. The Hassel is thickest, reaching 120 m, in the South Coast section [Figure 2.9]. Lithology is predominantly fine to very coarse quartzose sandstone. Planar features range from laminae to bedsets. In several outcrops the sandstones are heavily cross-bedded. Coal seams in the Hassel Formation are found near the town of Pond Inlet on Baffin Island.

2.52 Kanguk Formation

The Kanguk Formation unconformably overlies the Hassel Formation. Miall et al. (1980) distinguished two informal members [Table 2.1]. Sparkes (1989) informally identified the Byam Martin and Sermilik formations [Table 2.1]. This thesis uses the informal formation names from Sparkes (1989).

The Byam Martin formation [Sparkes 1989] roughly equates to the mudstone member of Miall et al. (1980) [Table 2.1] and unconformably overlies the Hassel Formation sands. The formation is a well lithified gray mudstone containing rare thin beds (1 to 10 cm) of white subarkosic sand. According to Sparkes (1989) it is common to find mudstone rip-up clasts and flame structures in the subarkosic sand beds.

The Sermilik formation of Sparkes (1989) equates with the sandstone member of Miall et al. (1980). Sparkes (1989) identified three distinct lithological units (lithotypes) in the Sermilik formation. The first lithotype is a 316-m-thick unit of well-sorted, medium- to very coarse-grained, buff to gray, subarkosic sandstone. The scale of bedding ranges from centimetre to ten metres thick [Sparkes 1989]. The second lithotype is a 156-m-thick unit of poorly consolidated subarkosic sandstone. The sands here are green to buff with lenticular bedding. Beds are predominantly tens of centimetres thick, but can reach metre scale. The third lithotype is gray, subarkosic, coarse-grained, matrix-supported conglomerate.

2.53 Eureka Sound Formation

In Eclipse Trough the Eureka Sound Formation unconformably overlies the Sermilik formation. Miall et al. (1980) divided the Eureka Sound Formation into four members, while Waterfield (1989) identified four informal formations that do not directly equate to the Miall et al. (1980) members [Table 2.1]. The four formations described by Waterfield (1989) are the Bylot Island, Pond Inlet, Navy board, and Aktineq formations.

The Bylot Island formation has contacts with the underlying Sermilik and Byam Martin formations. At the South Coast section the Bylot Island formation has a gradational contact with the Sermilik formation. At Twosnout Creek the Bylot Island formation has a sharp and conformable contact with the underlying Byam Martin formation. The formation consists of black mudstone and siltstone. Thin beds (2 to 50 cm) of fine- to medium-grained sandstone occur sporadically. The bases of the sand beds are erosional and contain rip-up clasts and flame structures.

The Pond Inlet formation conformably overlies the Bylot Island formation. The contact at the South Coast section is gradational over a thickness of 5 m and has a coarsening-upward succession of interbedded sands and silty shales. At the South Coast section the Pond Inlet formation equates to the upper sandstone member that Miall et al. (1980) described. At Twosnout Creek the Pond Inlet formation correlates to the lower sandstone member Miall et al.

(1980) described. The Pond Inlet formation is a sandstone containing minor conglomerates and siltstones. Two sandstone lithotypes occur throughout the formation; a white quartzose sandstone and a rare arkosic sandstone. The white sandstone is the only lithotype at Twosnout Creek and is the dominant lithotype at the South Coast section. Sandstone beds fine upwards and range in size from centimetres to tens of metres. Thin mudstone beds also range in size from centimetres to tens of metres, but they are never thicker than the bounding sandstone beds.

The Navy Board formation overlies the Pond Inlet formation with sharp and gradational contacts, depending on location. In localities where the contact is gradational the Navy Board formation consists of approximately 20 m of white sandstone fining upwards to black shale. Measured outcrop thickness of the Navy Board formation is 365 m. The Navy Board formation is a massive, unstructured to laminated black shale that contains thin gray sandstone beds. The sandstone beds fine upwards. The formation becomes coarser near the top of the section, where stacked beds of sandstone fining into siltstone are found. Overall the beds in the Navy Board formation show a coarsening-upward trend.

The Aktineq formation conformably overlies the Navy Board formation with a sharp contact. A change from dark gray coarsening up cycles to brown fining-up cycles marks the contact. The Aktineq formation sands and silts have fining- and thinning-upward cycles.   These cycles reach several tens of metres thick. Individual beds in the cycles fine upward from sandstone to siltstone and range from centimetres to metres in thickness [Waterfield 1989]. Planar lamination, flame structures, ripples, and cross stratification are common structures found in the Aktineq formation.

The samples collected by the Memorial group come from Late Cretaceous and Paleogene strata. It is not clear which stratigraphic units the Late Cretaceous samples were taken from, but the Paleogene samples were taken from the Pond Inlet formation.

3.0 Methodology

3.10 Processing

Processing palynological samples is a complex procedure that requires separating microscopic organic-walled fossils from consolidated sediments. Density of palynomorphs in the sediment is typically low and the palynomorphs must be concentrated for observation under the microscope [de Vernal et al 2010]. Concentrating the palynomorphs requires mechanical and chemical processes. The samples collected by Burden, Sparkes, and Waterfield were taken from freshly exposed outcrop limiting contamination. Subsequent to the thesis work by the Memorial group, the remaining raw samples were given to the GSCA, who had them processed for palynology, in part at GSC Calgary and in part by a private laboratory, Global Geolab Limited, in Medicine Hat, Alberta.

Linda Dancey [GSC Calgary; personal communication] provided the following processing criteria at GSC Calgary and Global Geolab Limited, which is broadly based on techniques outlined by Barss and Williams (1973) [Figure 3.1]. Each sample is digested in 25% hydrochloric acid (HCl) until the resulting reaction was complete. HCl is used to remove any carbonates present in the samples. HCl is then removed by settling and decanting the mixture with distilled water. The samples are then digested in hydrofluoric acid (HF), preferably on an oscillating plate. The HF will dissolve silicates in the sample. The HF requires centrifuging to remove it from the sample. Approximately 25 ml of concentrated HCl is added to the sample in a test tube, which is then placed in a hot water bath for 10 minutes, stirring occasionally. In order to remove the HCl the sample must be centrifuged twice. A heavy liquid separation process is done by adding 25 ml of zinc bromide and centrifuging for 20 minutes. The top portion of the test tube is decanted off then the sample is centrifuged five or six times to remove the zinc bromide. A small portion of the test tube residue is then sieved to remove +150 µm and -10 µm fractions. This portion is smeared on two coverslips that are mounted on a slide labelled 'K' for kerogen. Coverslips are 22 x 40 mm and are then mounted on glass slides. The remaining residue is oxidized using Schulze solution, which is an oxidizing mixture of $KClO_3$ and HNO_3. Once oxidized the residue is neutralized with 10% ammonium hydroxide (NH_4OH) then washed. The sample is then sieved to remove the +150 µm and -10 µm fractions and is stained with Safranin red to increase palynomorph visibility. The test tube is once again centrifuged to remove any excess stain. A portion of this residue is smeared on a coverslip and reads 'UN' for unsieved slides. The remaining residue is sieved with 45 and 20 µm sieves creating +45, +20, and -20 fractions. Each fraction is smeared onto two coverslips and the slides labelled accordingly. Once all the coverslips have dried they are inverted and mounted onto glass slides. Glass slides are 25 x 74 mm and always contain a label on the left edge [Barss and Williams 1974].

3.20 Instruments

I analysed the samples at the GSC Atlantic (at the Bedford Institute of Oceanography) in Dartmouth, Nova Scotia. I used the Nikon Ds-Fi2 microscope provided by GSCA. The camera I used for photographs was the Nikon Digital Sight DS-U3. I performed phase contrast, oil immersion, and interference contrast analysis in the identification and photographing processes. I annotated the photographs using the image capture program NIS-Elements BR.

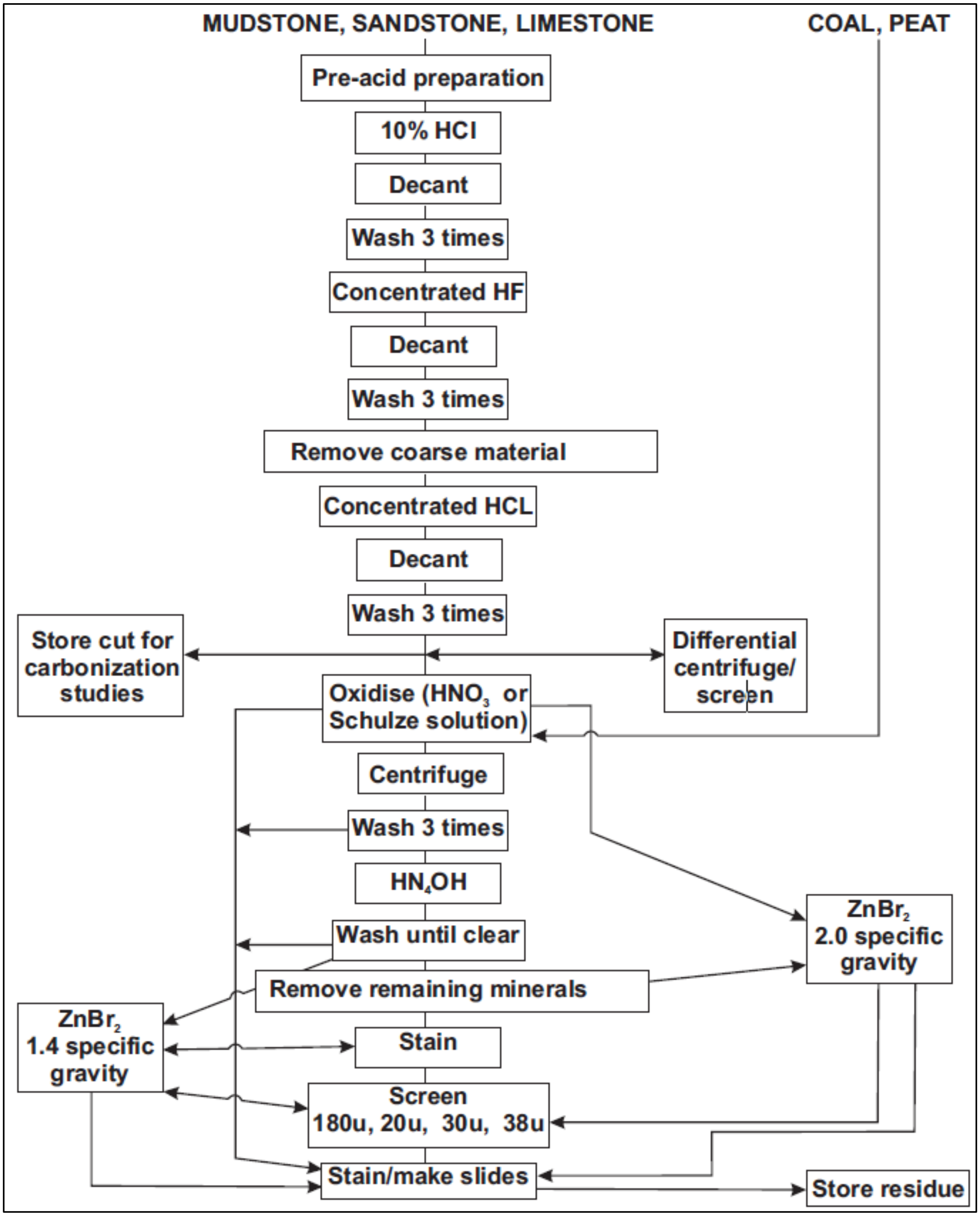

Figure 3.1 - Flowchart depicting standard processing techniques [from Nøhr-Hansen et al. in press]

3.30 Palynological analysis

Determining the best samples to analyse was the first step in my palynological analysis. The samples collected by Sparkes (1989) and Waterfield (1989) produced 63 samples from 21 sections. Each sample was split into six sieve fractions. I analysed 14 samples from five sections that, according to Sparkes (1989) and Waterfield (1989), straddle the Cretaceous-Paleogene boundary. I chose samples based on two major criteria, stratigraphic importance and the potential of each slide for palynological analysis. I wanted to analyse samples that would provide accurate palynological assemblages on either side of the Cretaceous-Paleogene boundary. I performed an initial reconnaissance of the slides to determine the slides with greatest potential for analysis. I graded each sample on abundance, preservation quality, and diversity. Abundance refers to the number of palynomorphs present in a slide. Preservation quality is the physical condition of the palynomorphs. Diversity is the number of different genera on a slide.

Once I chose the best samples, I began to identify the genera present in each one. I primarily used the +45 sieve fraction for my analysis. Beginning with the top-left portion of the coverslip I methodically worked down then across the coverslip. This back-and-forth traversing maximised the opportunity to find specimens efficiently. I photographed and attempted to identify any dinoflagellates I saw under the objective. I took clear and informative pictures to help identify the dinoflagellates without having a microscope, and its capabilities, readily available.

The first step in my identification process was to identify the key morphological features described in chapter 2.10. Once I identified these features I photographed them. Some dinocysts only required one photograph to capture these features, while others required multiple photographs using different optics and/or focal levels. The archeopyle was the most important feature to capture and identify because in most dinocysts it is the only indicator of tabulation. Determining whether the archeopyle was apical, precingular, or intercalary can be difficult as, being organic-walled, dinocysts are easily distorted or torn. I also focused on capturing the nature of processes and ornamentation on dinocysts. Dinoflagellate processes are diverse and can help distinguish between genera with the same or similar tabulation.

The proportion of miospores to dinocysts in each sample is used in paleoenvironmental analysis. I completed a sample count to determine the proportions in my 14 samples. I counted miospores, bisaccate pollen, gonyaulacoids, peridinioids, and any unknown dinocysts using the unsieved slide (UN). I counted until I reached 100 total palynomorphs to get an accurate representation of the entire sample. I determined the palynological assemblages and sample counts to ensure I gathered as much biostratigraphic information as possible.

Figures 3.2 and 3.3 show all 14 samples and their location on the sections. The geographic locations of the sections can be found in Appendix A. Sparkes (1989) and Waterfield (1989) interpreted the sections in Figure 3.2 as Late Cretaceous and both sections in Figure 3.31 as Paleocene. It is not clear which stratigraphic units the samples in Figure 3.30 were taken from. The samples in Figure 3.3 were taken from the Pond Inlet formation.

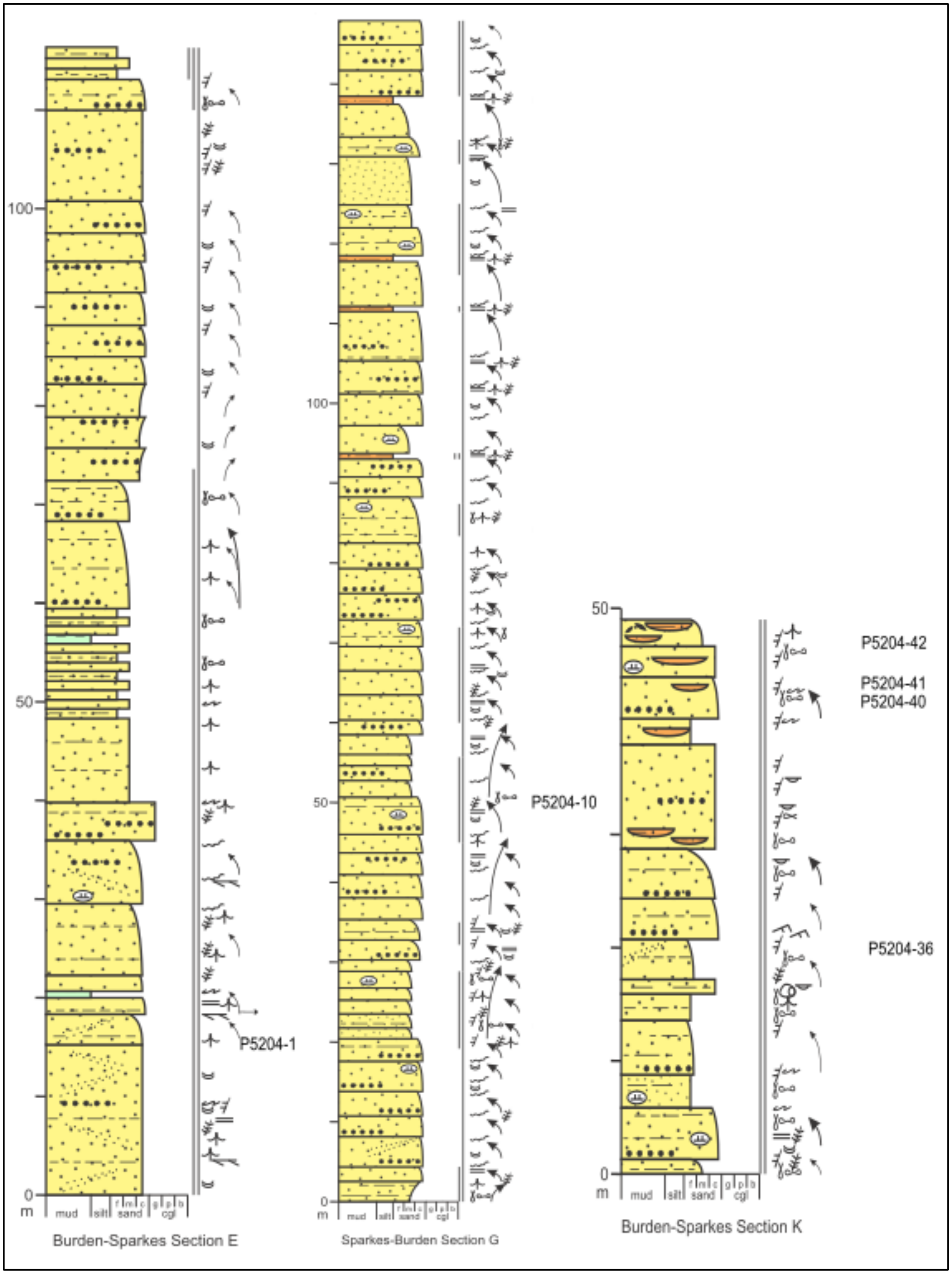

Figure 3.2 – Cretaceous sections E, G, and K

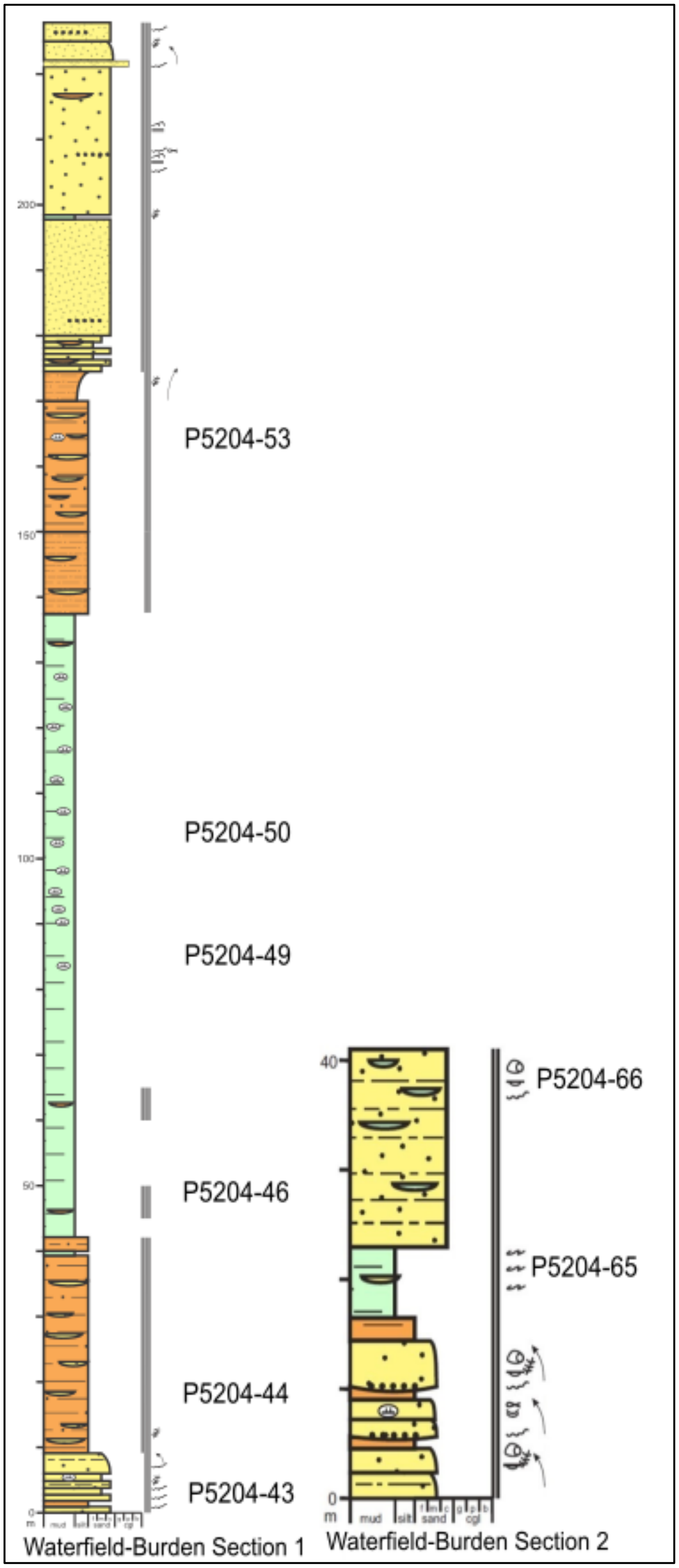

Figure 3.3 - Paleocene sections 1 and 2

4.0 Plates

Included here are five plates showing 100 palynomorphs found across the 14 samples I analysed. Plates are organised, for the most part, in alphabetical order according to genus then species. Informal (unpublished) names are in quotes.

Plate 1

Scale bar represents 20 µm [all figures].

Figure 1. *Alterbidinium "gigantium"*, dorsal view
Figure 2. *Alterbidinium "gigantium"*, ventral view in phase contrast
Figure 3. *Apteodinium sp*, left lateral view
Figure 4. *Areoligera sp*
Figure 5. *Areoligera volata*, dorsal view
Figure 6. "*Cassiculodinium reterum"*, ventral view
Figure 7. "*Cassiculodinium reterum"*, oblique apical view
Figure 8. "*Cassiculodinium reterum"*, ventral view
Figure 9. *Cerodinium diebelii*
Figure 10. *Cerodinium diebelii*
Figure 11. *Cerodinium diebelii*
Figure 12. *Cerodinium diebelii*
Figure 13. *Cerodinium kangiliense*
Figure 14. *Cerodinium kangiliense*
Figure 15. *Cerodinium kangiliense*
Figure 16. *Cerodinium sp*
Figure 17. *Chatangiella tripartita*, dorsal surface
Figure 18. *Chatangiella tripartita*, dorsal surface
Figure 19. *Chatangiella victoriensis*, dorsal surface
Figure 20. *Chatangiella victoriensis*, dorsal surface

Plate 2

Scale bar represents 20 µm in all figures.

Figure 1. *Chatangiella victoriensis*, dorsal surface

Figure 2. *Chatangiella victoriensis*, ventral surface

Figure 3. *Cordosphaeridium delimurum*, right lateral view

Figure 4. *Cordosphaeridium fibrospinosum*,

Figure 5. *Cribroperidinium spp*, right lateral view

Figure 6. *Cribroperidinium spp*

Figure 7. *Cyclonephelium cf. compactum*, ventral view

Figure 8. *Deflandrea borealis*, dorsal view

Figure 9. *Deflandrea borealis*, dorsal view, same specimen as Figure 8 in phase contrast

Figure 10. "*Deltiella harena"*, ventral surface

Figure 11. "*Deltiella harena"*

Figure 12. "*Deltiella scuta"*, dorsal surface

Figure 13. "*Deltiella scuta"*, dorsal surface, same specimen as Figure 12.

Figure 14. "*Deltiella cava"*, dorsal surface

Figure 15. "*Deltiella cava"*, dorsal surface, same specimen as Figure 12 in phase contrast

Figure 16. "*Echinodinium" cf. compactum*, ventral view

Figure 17. "*Echinodinium cornupilosum"*, dorsal view

Figure 18. "*Echinodinium cornupilosum"*, dorsal view, same specimen as Figure 17.

Figure 19. *Exochosphaeridium bifidum*, left lateral view

Figure 20. *Florentinia sp*, ventral view

Plate 3

Scale bar represents 20 µm in all figures.

Figure 1. *Florentinia sp*, left lateral view

Figure 2. *Heterosphaeridium difficile*

Figure 3. *Heterosphaeridium difficile*, same specimen as Figure 2

Figure 4. *Heterosphaeridium difficile*

Figure 5. *Heterosphaeridium*, *difficile*

Figure 6. *Heterosphaeridium*, *difficile*, specimen shows strong evidence of reworking

Figure 7. *Heterosphaeridium sp*

Figure 8. *Hystrichosphaeridium quadratum*

Figure 9. *Hystrichosphaeridium quadratum*

Figure 10. *Hystrichosphaeridium quadratum*

Figure 11. *Hystrichosphaeridium quadratum*

Figure 12. *Hystrichosphaeridium quadratum*

Figure 13. *Hystrichosphaeridium quadratum*, same specimen as Figure 12 in phase contrast

Figure 14. *Hystrichosphaeridium quadratum*

Figure 15. *Hystrichosphaeridium quadratum*

Figure 16. *Hystrichosphaeridium quadratum*

Figure 17. *Hystrichosphaeridium quadratum*

Figure 18. *Kleithriasphaeridium loffrense*

Figure 19. *Kleithriasphaeridium loffrense*, right lateral view

Figure 20. *Kleithriasphaeridium loffrense*, dorsal view

Plate 4

Scale bar represents 20 µm in all figures.

Figure 1. *Kleithriasphaeridium sp*

Figure 2. *Kleithriasphaeridium sp*

Figure 3. *Lingulodinium sp*

Figure 4. *Luxadinium sp*, dorsal view

Figure 5. *Luxadinium sp*, dorsal view

Figure 6. *Manumiella coronate*, dorsal view

Figure 7. *Odontochitina spp*

Figure 8. *Odontochitina spp*

Figure 9. *Palaeocystodinium bulliforme*

Figure 10. *Palaeocystodinium golzowense*, oblique right dorsal view

Figure 11. *Palaeocystodinium golzowense*, oblique left dorsal view

Figure 12. *Palaeocystodinium golzowense*, right lateral view

Figure 13. *Palaeoperidinium pyrophorum*

Figure 14. *Palaeoperidinium pyrophorum*

Figure 15. *Palaeoperidinium pyrophorum*

Figure 16. *Palaeoperidinium pyrophorum*

Figure 17. *Palaeoperidinium pyrophorum*

Figure 18. *Palaeoperidinium pyrophorum*

Figure 19. *Pervosphaeridium sp*, left lateral view

Figure 20. *Sentusidinium spp*, dorsal view

Plate 5

Scale bar represents 20 µm in all figures.

Figure 1. *Spiniferites spp*

Figure 2. *Achomosphaera ramulifera*,

Figure 3. *Spiniferites spp*

Figure 4. *Spiniferites spp*

Figure 5. *Spongodinium delitiense*, oblique left dorsal view

Figure 6. *Spongodinium delitiense*, right lateral view

Figure 7. *Spongodinium delitiense*, apical view

Figure 8. *Spongodinium delitiense*, apical view

Figure 9. *Spongodinium delitiense*, dorsal view

Figure 10. *"Tenua distinctum"*, ventral view in phase contrast

Figure 11. *Thalassiphora pelagica*, dorsal view

Figure 12. *Thalassiphora pelagica*, left lateral view

Figure 13. *Trithyrodinium evittii*, dorsal view

Figure 14. *Trithyrodinium evittii*, dorsal view

Figure 15. *Trithyrodinium evittii*, dorsal view

Figure 16. Bisaccate

Figure 17. Bisaccate

Figure 18. Trilete fern spore

Figure 19. Trilete fern spore

Figure 20. Triporate angiosperm spore

Plate 1

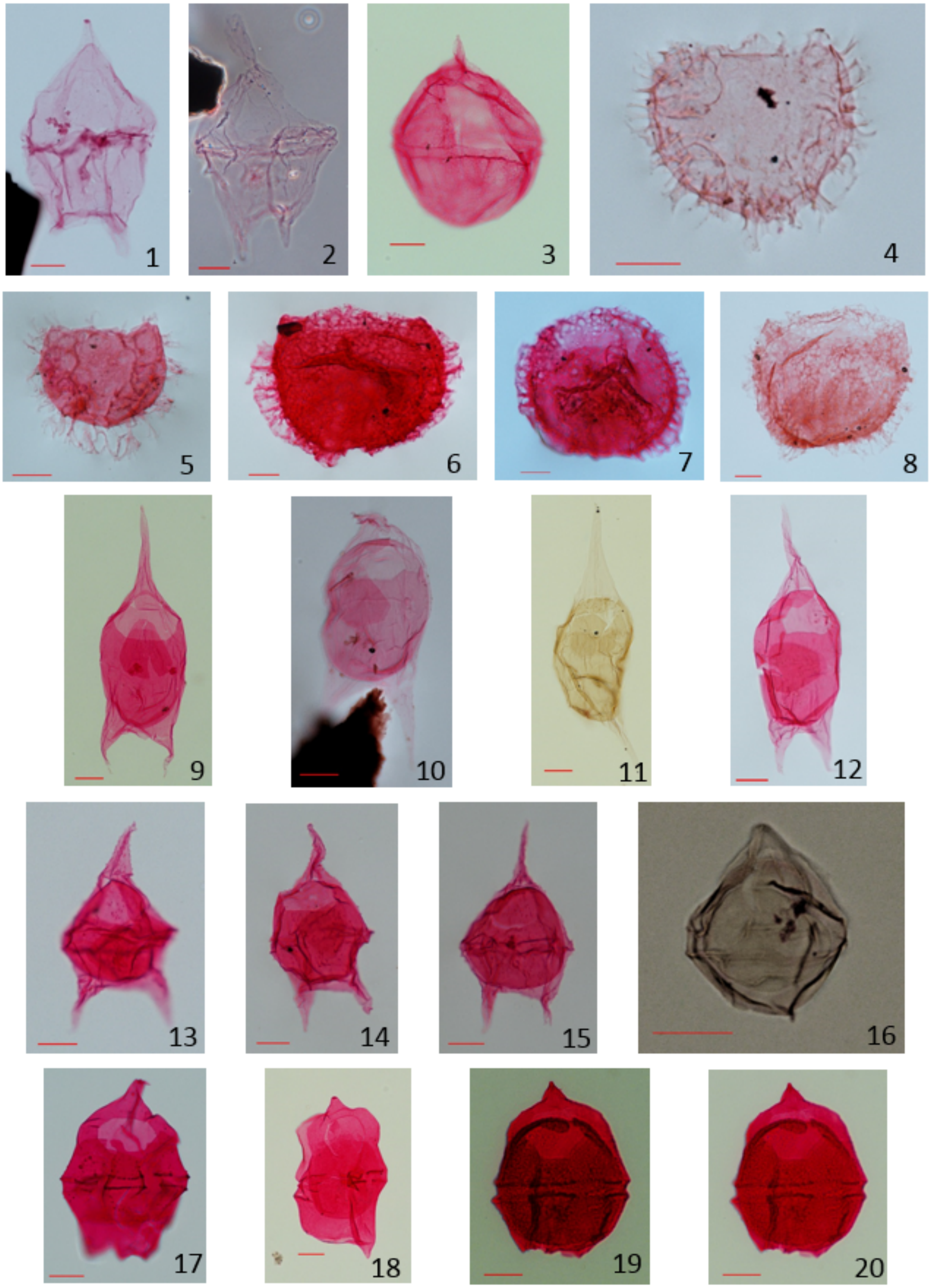

Plate 2

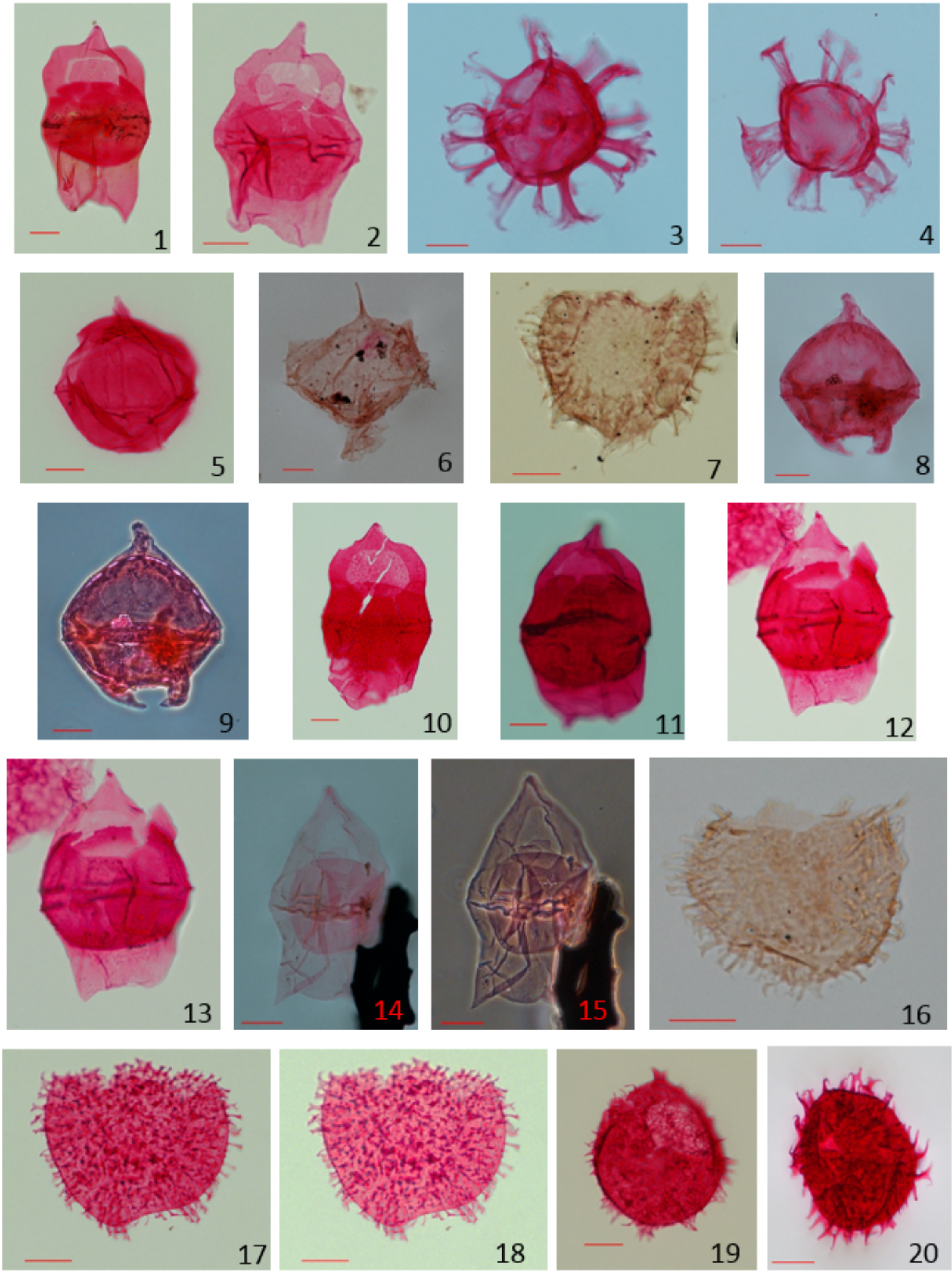

Plate 3

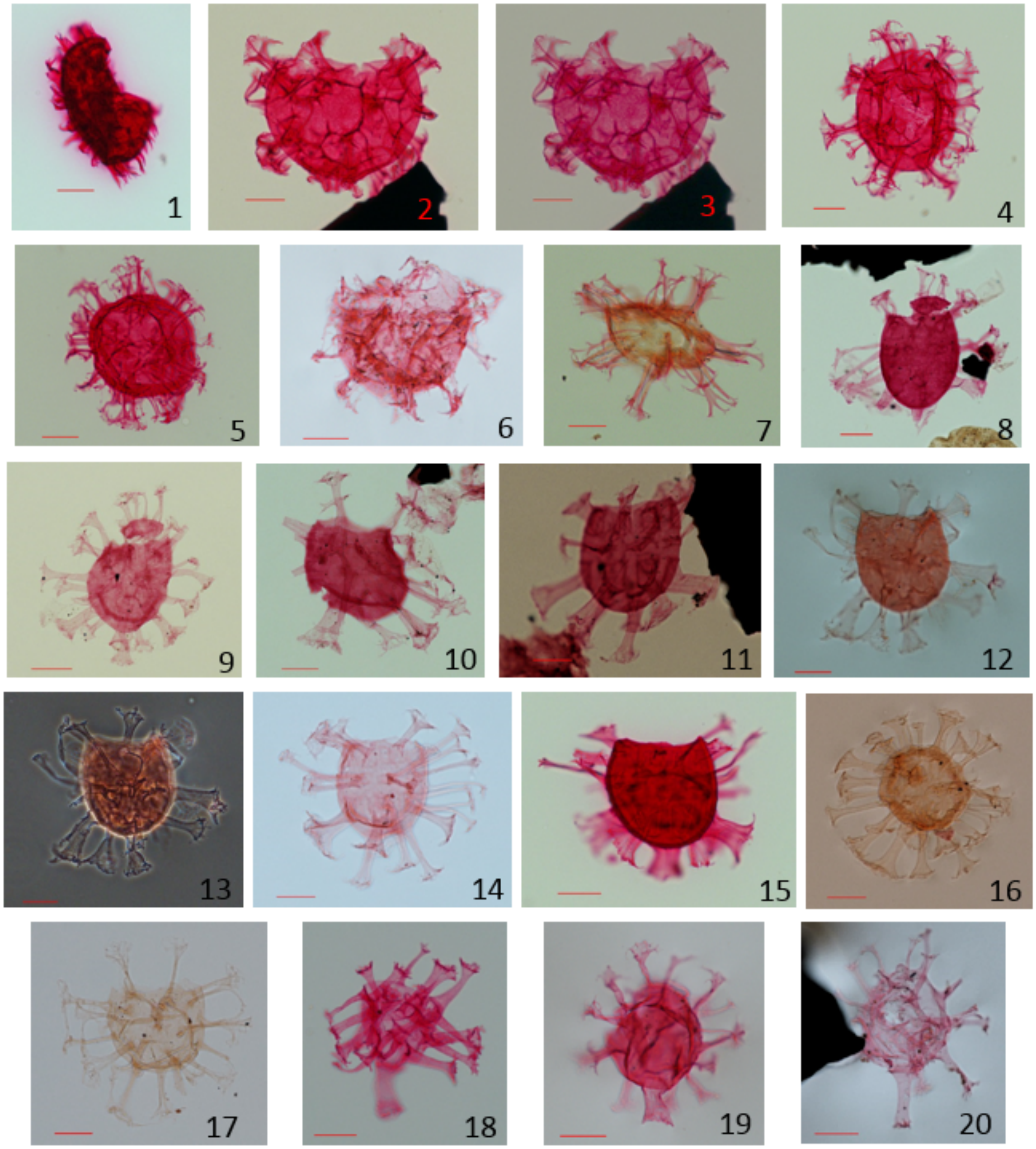

Plate 4

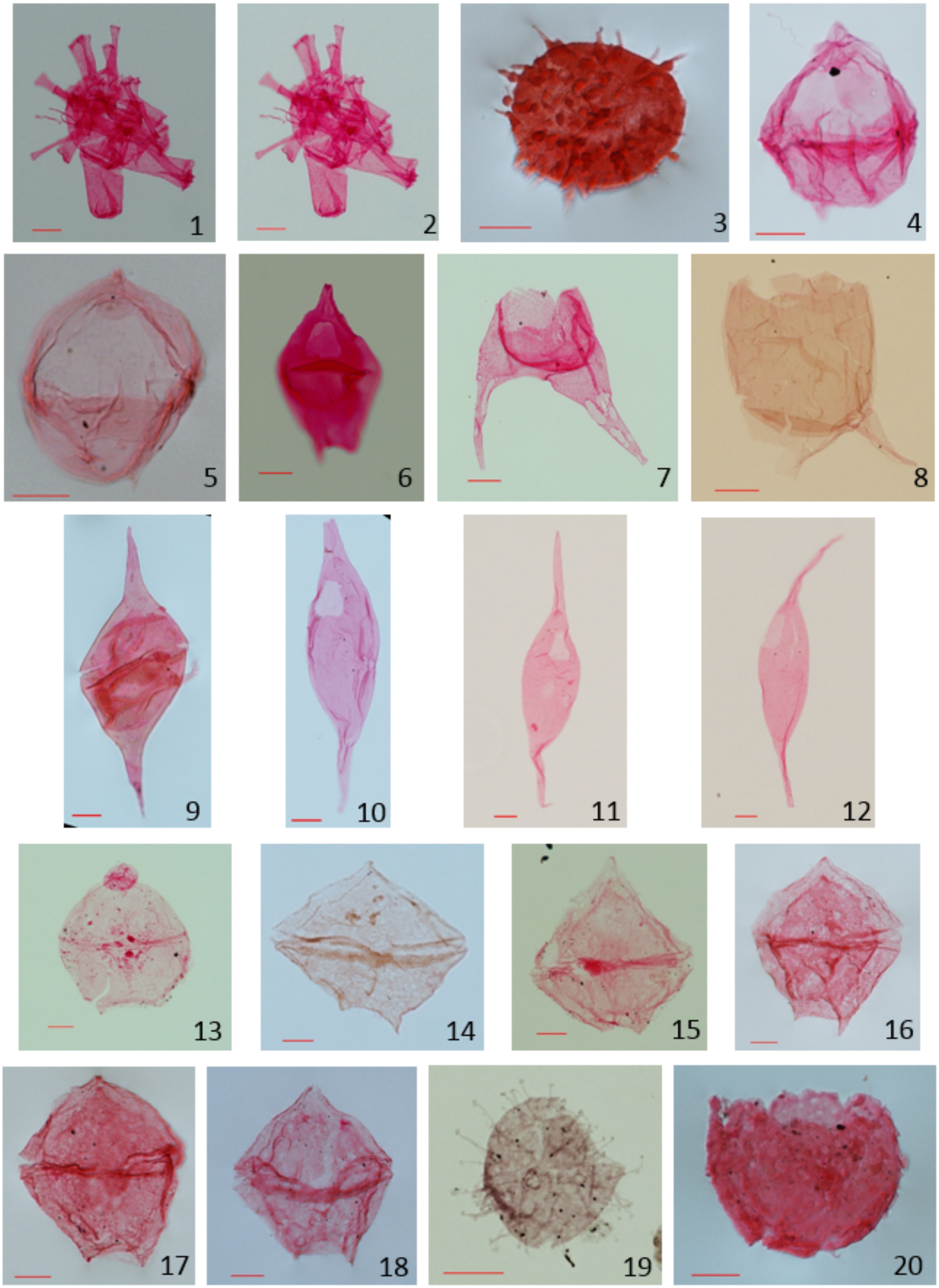

Plate 5

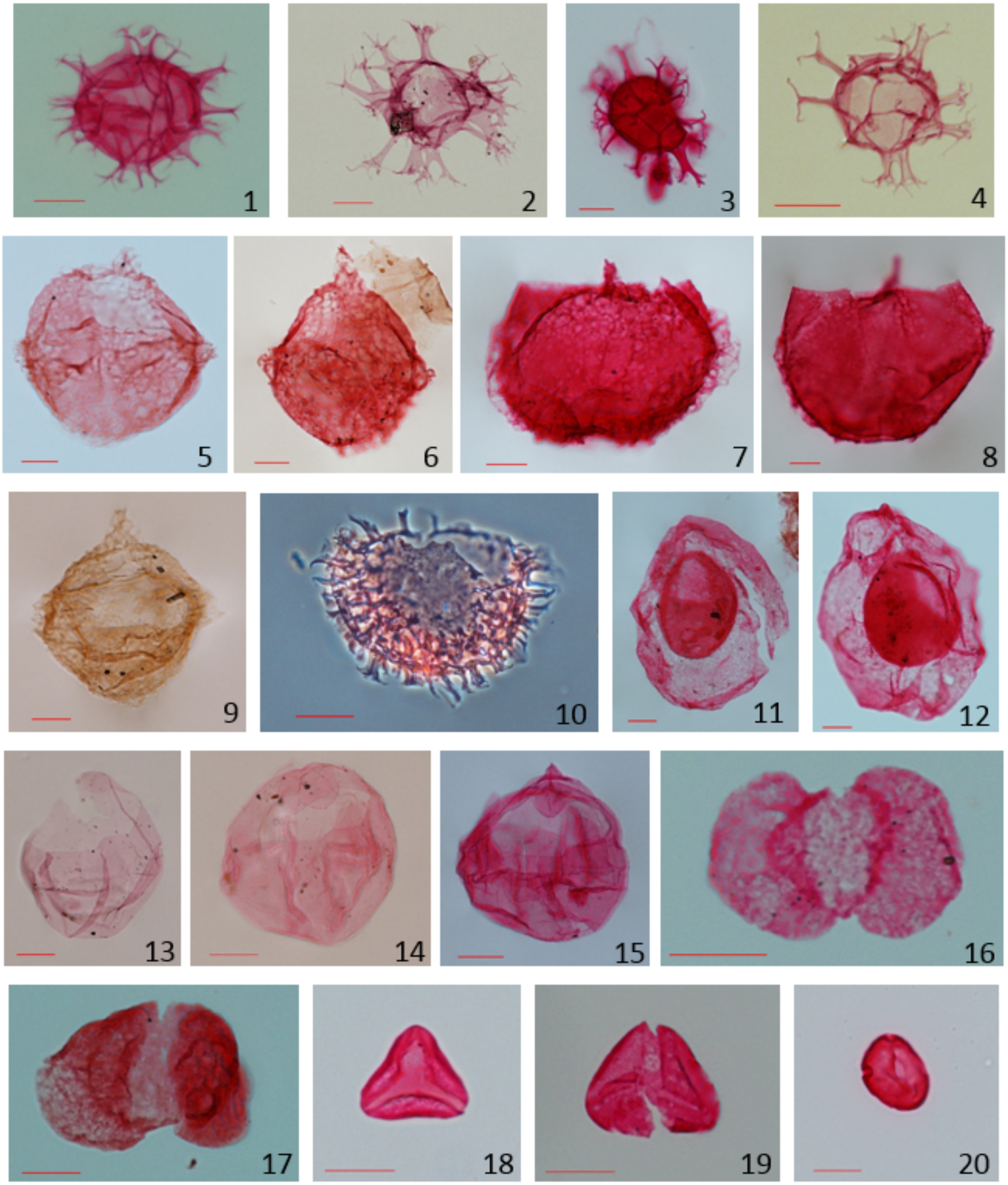

5.0 Biostratigraphy results and discussion

Table 5.1 – First occurrence plot

Sample	P5204-01	P5204-10	P5204-36	P5204-40	P5204-41	P5204-42	P5204-43	P5204-44	P5204-46	P5204-49	P5204-50	P5204-53	P5204-65	P5204-66
Chatangiella tripartita	■	■												
Chatangiella victoriensis	■	■	■	■										
Deltiella "harena"	■	■												
Deltiella "scuta"	■	■							■	■				
Florentinia spp.	■													
Heterosphaeridium difficile	■	■	■											
Kleithriasphaeridium loffrense	■	■					■					■		
Spiniferites spp.	■	■		■	■	■						■		
Apteodinium sp.		■												
"Echinodinium" "cornupilosum"		■												
Exochosphaeridium bifidum		■												
Kleithriasphaeridium sp.		■												
Manumiella coronata		■												
Odontochitina spp.		■				■								
Palaeoperidinium pyrophorum		■		■	■	■		■	■	■	■	■	■	■
Cerodinium diebelii			■	■	■	■	■		■	■	■	■		
Cribroperidinium spp.			■					■						
Hystrichosphaeridium quadratum			■	■	■	■	■	■	■	■	■	■	■	■
Spongodinium delitiense			■					■	■	■	■	■		
Cerodinium sp.				■										
Heterosphaeridium sp.					■									
Cyclonephelium cf. compactum						■								
Pervosphaeridium sp.						■								
Areoligera spp.							■						■	
Deltiella "cava"							■							
Achomosphaera ramulifera								■						
Lingulodinium sp.								■						
Palaeocystodinium golzowense								■		■	■		■	
Tenua distinctum								■						
Thalassiphora pelagica								■					■	■
Alterbidinium "gigantium"									■	■				
"Echinodinium" cf. compactum									■					
Luxadinium sp.									■		■			
Sentusidinium spp.									■				■	
Trithyrodinium evittii									■	■	■			■
Cassiculodinium "reterum"										■	■			
Phelodinium kozlowskii										■	■			
Cerodinium kangiliense												■	■	■
Deflandrea borealis													■	
Palaeocystodinium bulliforme													■	
Areoligera volata														■
Cordosphaeridium delimurum														■
Cordosphaeridium fibrospinosum														■

Table 5.2 – Last occurrence plot

P5204-01	P5204-10	P5204-36	P5204-40	P5204-41	P5204-42	P5204-43	P5204-44	P5204-46	P5204-49	P5204-50	P5204-53	P5204-65	P5204-66	Sample
■														*Florentinia* spp.
	■													*Apteodinium* sp.
■	■													*Chatangiella tripartita*
■	■													*"Deltiella harena"*
	■													*"Echinodinium cornupilosum"*
	■													*Exochosphaeridium bifidum*
	■													*Kleithriasphaeridium* sp.
	■													*Manumiella coronata*
■	■	■												*Heterosphaeridium difficile*
			■											*Cerodinium* sp.
■	■	■	■											*Chatangiella victoriensis*
				■										*Heterosphaeridium* sp.
					■									*Cyclonephelium cf. compactum*
	■				■									*Odontochitina* spp.
					■									*Pervosphaeridium* sp.
						■								*"Deltiella cava"*
							■							*Achomosphaera ramulifera*
		■					■							*Cribroperidinium* spp.
							■							*Lingulodinium* sp.
							■							*Tenua distinctum*
								■						*"Echinodinium" cf. compactum*
								■	■					*Alterbidinium "gigantium"*
■	■							■	■					*"Deltiella scuta"*
									■	■				*Cassiculodinium "reterum"*
								■		■				*Luxadinium* sp.
									■	■				*Phelodinium kozlowskii*
		■	■	■	■	■		■	■	■	■			*Cerodinium diebelii*
■	■					■					■			*Kleithriasphaeridium loffrense*
■	■		■	■	■						■			*Spiniferites* spp.
		■					■	■	■	■	■			*Spongodinium delitiense*
						■						■		*Areoligera* spp.
												■		*Deflandrea borealis*
												■		*Palaeocystodinium bulliforme*
							■		■	■		■		*Palaeocystodinium golzowense*
								■				■		*Scentusidinium* spp.
													■	*Areoligera volata*
											■	■	■	*Cerodinium kangiliense*
													■	*Cordosphaeridium delimurum*
													■	*Cordosphaeridium fibrospinosum*
		■	■	■	■	■	■	■	■	■	■	■	■	*Hystrichosphaeridium quadratum*
	■		■	■	■		■	■	■	■	■	■	■	*Palaeoperidinium pyrophorum*
							■					■	■	*Thalassiphora pelagica*
								■	■	■			■	*Trithyrodinium evittii*

The taxa listed in Table 5.1 are organized according to first occurrence (FO) and the taxa in Table 5.1 are organized according to last occurrence (LO). Organizing the assemblages based on first and last occurrences enhances first and last appearances of key biostratigraphic taxa in the palynological assemblages. Many taxa in each sample do not provide useful biostratigraphic information. For clarity, the discussion only includes key biostratigraphic taxa that are used in determining the ages, not the entire palynological assemblages.

The samples from sections E and G (P5204-1 and P5204-10) have the same key biostratigraphic taxa in their palynological assemblages [Table 5.1 and Table 5.2]. *Heterosphaeridium difficile* (LO Early Santonian) defines the age constraints for these sections. These sections are Coniacian to Early Santonian in age [Figure 5.1].

The samples from section K (P5204-36, P5204-40, P5204-41, and P5204-42) and lower section 1 (P5204-43 and P5204-44) have the same, or similar, key taxa [Table 5.1 and Table 5.2]. While the presence of *Heterosphaeridium difficile* in sample P5204-36 suggests a minimum Early Santonian age, the first appearance of *Cerodinium diebelii* (FO Early Maastrichtian) in sample P5204-36 is more reliable as a biostratigraphic indicator. The age determined from a FO is more accurate than the age determined by a LO. This is because specimens may be reworked higher up the section effectively skewing the biostratigraphic age. The presence of *Tenua distinctum* and *Thalassiphora pelagica* in sample P5204-44 provide the age top for these samples. *Tenua distinctum* does not cross the Cretaceous-Paleogene boundary, while *Thalassiphora pelagica* (FO Late Maastrichtian) puts the base of P5204-44 in the Late Maastrichtian. These samples are Early Maastrichtian to Late Maastrichtian in age [Figure 5.1 and Figure 5.2].

The samples from the middle of section 1 (P5204-46, P5204-49, and P5204-50) have the same key taxa [Table 5.1 and Table 5.2]. The age base for these samples comes from the palynological assemblage in sample P5204-44. *Spongodinium delitiense* (LO 64 Ma in the Danian) provides the age top for these samples. These samples are Late Maastrichtian to Early Danian (64 Ma). The Cretaceous-Paleogene boundary is located somewhere amongst these samples in the middle of section 2 [Figure 5.2].

The age base of the sample from the top of section 2 (P5204-53) is defined by *Cerodinium kangiliense* (FO Danian). The age top is defined by *Cerodinium diebelii* (LO Danian-Selandian boundary). This sample is Danian in age.

The samples in section 2 (P5204-65 and P5204-66) have the same key biostratigraphic taxa in their palynological assemblages [Table 5.10 and Table 5.11]. *Palaeocystodinium bulliforme* (FO Early Selandian) provides the age base for these samples. *Hystrichosphaeridium quadratum* (LO Selandian) provides the age top for these samples. The samples in section 2 are Selandian in age [Figure 5.2].

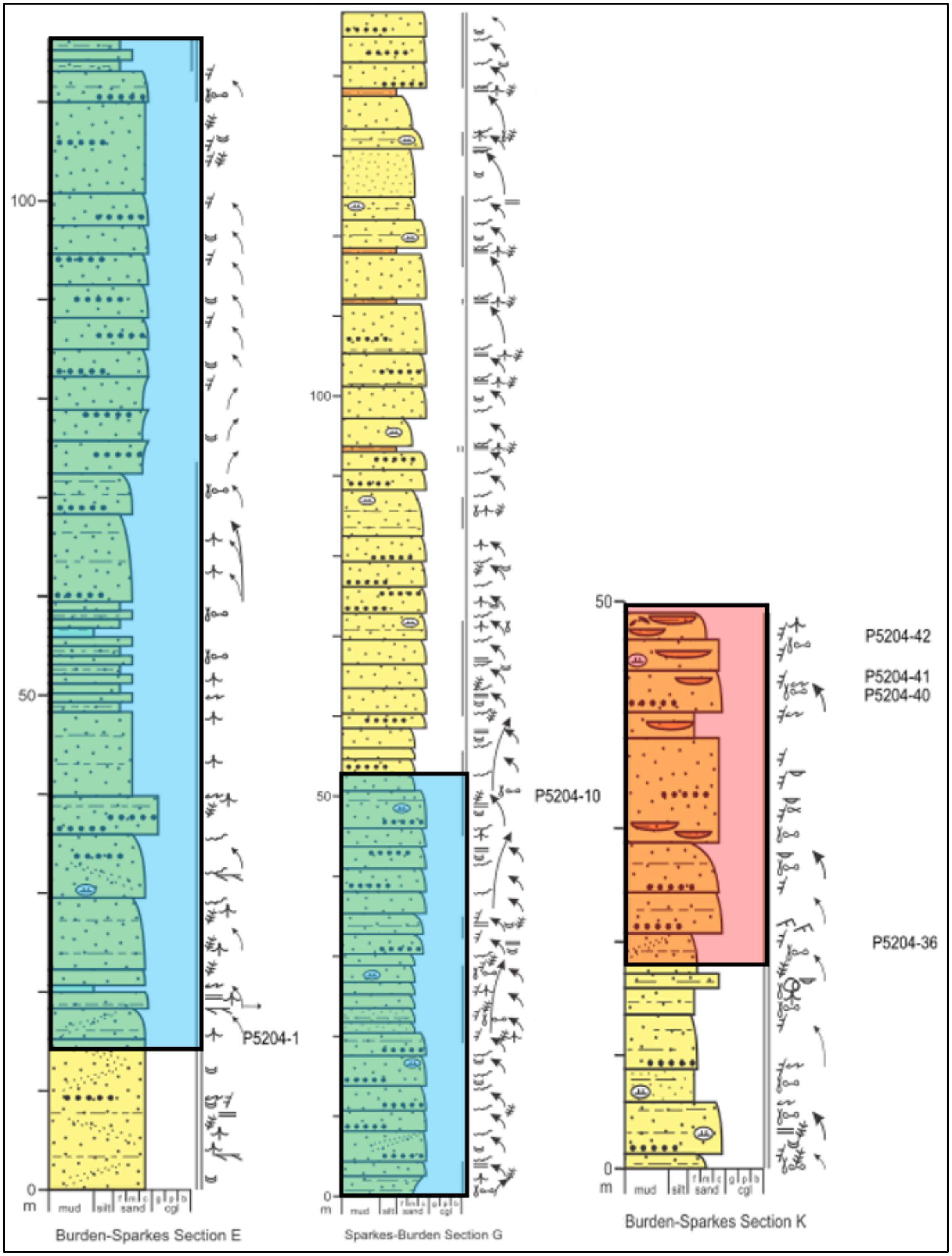

Figure 5.1 – Biostratigraphic ages plotted on sections. **Blue)** Coniacian – Early Santonian. **Red)** Early Maastrichtian – Late Maastrichtian.

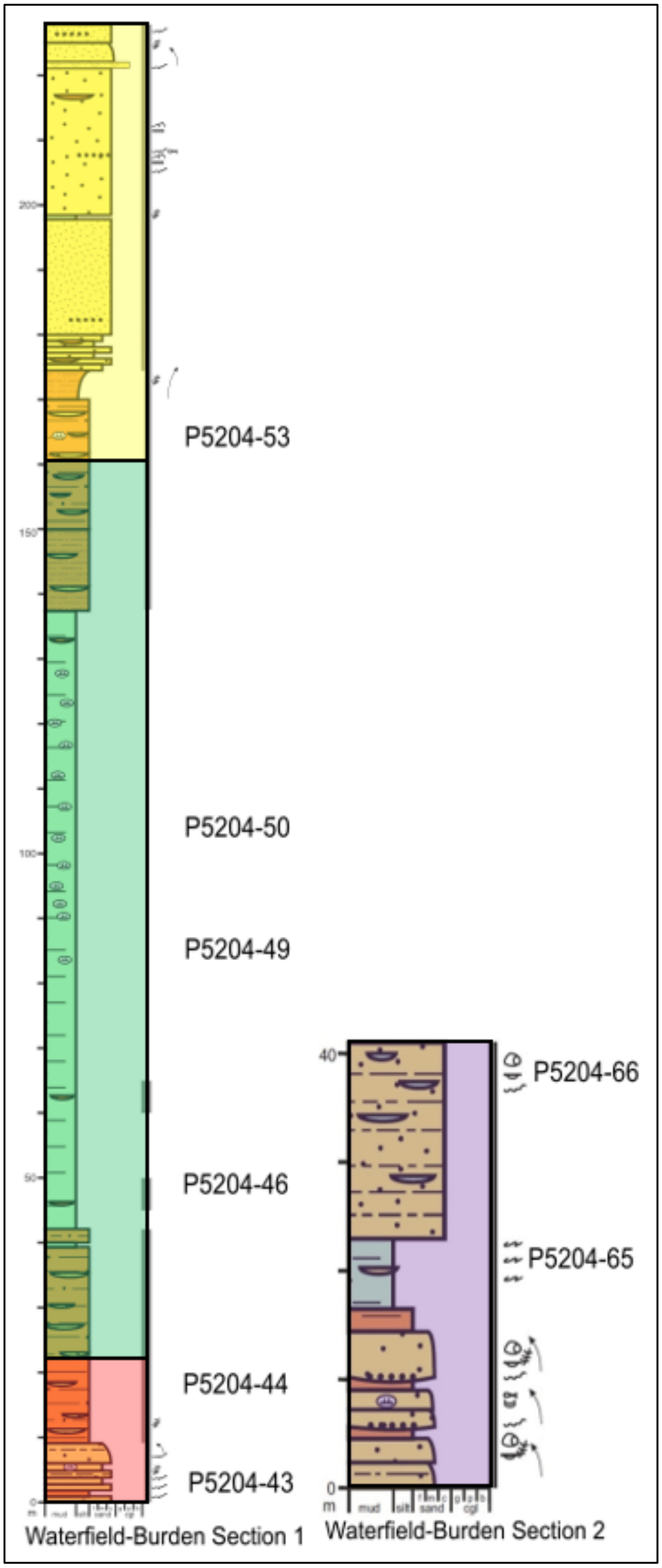

Figure 5.2 – Biostratigraphic ages plotted on sections. **Red)** Early Maastrichtian – Late Maastrichtian. **Green)** Location of Cretaceous-Paleogene Boundary. **Yellow)** Danian. **Purple)** Selandian.

6.0 Paleoenvironment results and discussion

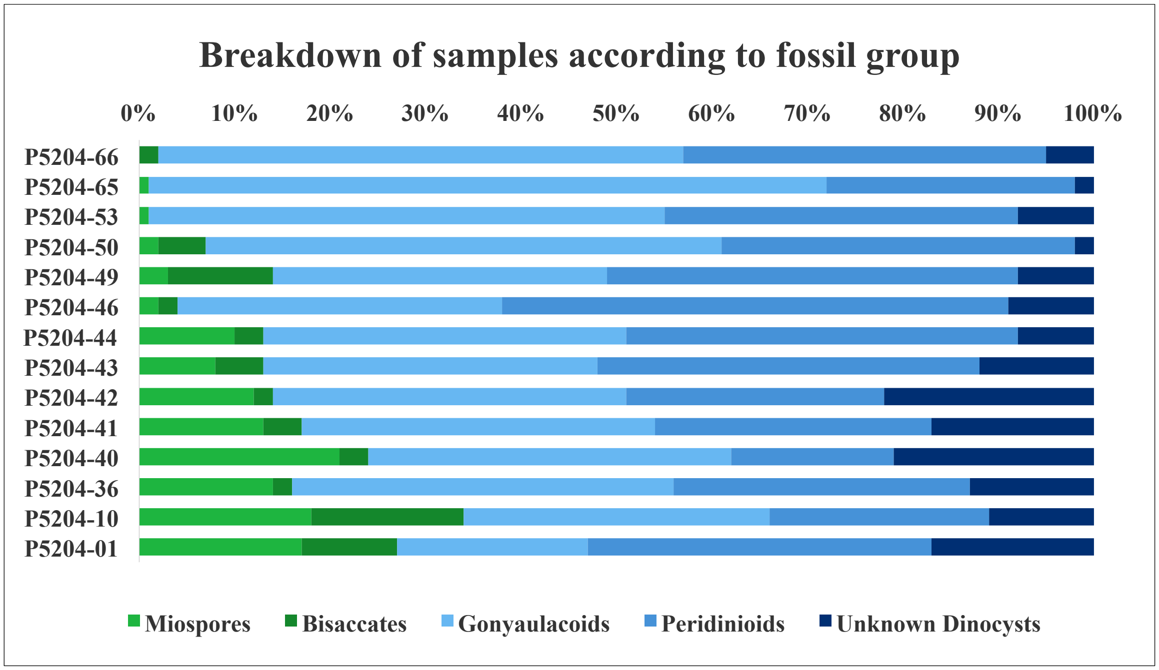

Figure 6.1 – Paleoenvironmental plot showing ratio of miospores **(green)** to dinocysts **(blue)**

Dinocysts dominate the palynological assemblages of all 14 samples [Figure 6.1]. The dinocysts [Figure 6.1 blue] represent marine environments whereas the miospores [Figure 6.1 green] derive from terrestrial environments. The dominance of dinocysts throughout the samples suggests a marine environment where distance from the coast is increasing up section (from section E to section 2). Samples are grouped following the paleoenvironment preferences of dinocyst taxa shown in Figure 6.2. Paleoenvironment for these samples is limited to inner and outer neritic zones. The neritic zone extends from the low tide level to the edge of the continental shelf. There is not a distinct physical boundary between inner and outer neritic zones.

The samples from sections E and G (P5204-01 and P5204-10, respectively) have the largest proportions of miospores relative to dinocysts [Figure 6.1], indicating they are the closest samples to the coast. The inner neritic preferring genus *Heterosphaeridium* is present in both samples whereas common outer neritic taxa [Figure 6.2] *Hystrichosphaeridium* and *Cerodinium* are not present. The presence of *Spiniferites* (an outer neritic preferring genus) in both samples suggests the paleoenvironment is inner neritic bordering on outer neritic.

The lower sample from section K (sample P5204-36) has dinocyst taxa that indicate both inner neritic and outer neritic paleoenvironments. *Cribroperidinium* and *Heterosphaeridium* are the genera present that have preferred inner neritic paleoenvironments [Figure 6.2]. *Cerodinium* and *Hystrichosphaeridium* are present and have outer neritic preferences. Within sample P5204-36 the outer neritic preferring genera (*Cerodinium* and *Hystrichosphaeridium*) are far more abundant than inner neritic preferring genera (*Cribroperidinium* and *Heterosphaeridium*). This suggests an outer neritic paleoenvironment that borders the inner neritic zone.

The palynological assemblages from the top of section K (samples P5204-40, P5204-41, and P5204-42) suggest an outer neritic paleoenvironment. The outer neritic genera *Cerodinium*, *Hystrichosphaeridium*, and *Spiniferites* are abundant in all three samples.

The palynological assemblages from lower section 1 (samples P5204-43 and P5204-44) suggest a paleoenvironment that borders the inner and outer neritic zones. Inner neritic preferring genera *Areoligera* (P5204-43) and *Cribroperidinium* (P5204-44) are present. Outer neritic preferring genera *Cerodinium* (P5204-43) and *Hystrichosphaeridium* (both samples) are also present. The presence of both inner and outer neritic preferring genera indicates that the paleoenvironment borders the inner and outer neritic zones.

The palynological assemblages from the remainder of section 1 (samples P5204-46, P5204-49, P5204-50, and P5204-53) suggest an outer neritic paleoenvironment. Outer neritic preferring genera *Cerodinium*, *Hystrichosphaeridium*, *Phelodinium* (P5204-49 and P5204-50), and *Spiniferites* (P5204-53) are present throughout the samples. No inner neritic taxa were found in the middle of section 1.

The samples from section 2 (P5204-65 and P5204-66) indicate an outer neritic paleoenvironment that is closer to the inner/outer neritic boundary than the samples from upper section 1. The outer neritic preferring genera *Cerodinium*, *Cordosphaeridium*, and *Hystrichosphaeridium* dominate the samples. The only inner neritic preferring genus *Areoligera* is sparse in sample P5204-65, but common in sample P5204-66.

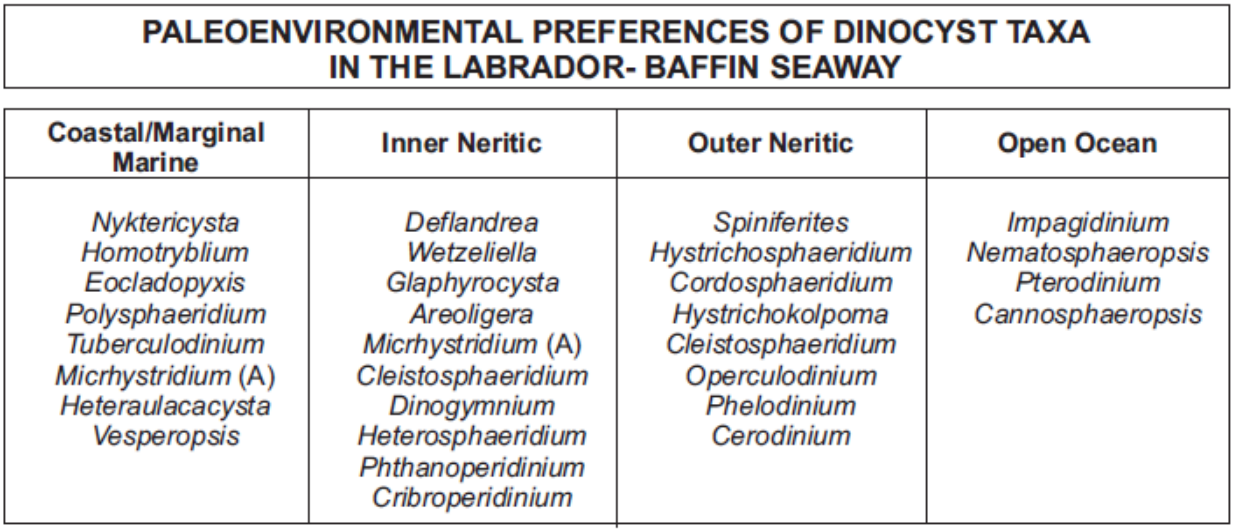

PALEOENVIRONMENTAL PREFERENCES OF DINOCYST TAXA IN THE LABRADOR- BAFFIN SEAWAY

Coastal/Marginal Marine	Inner Neritic	Outer Neritic	Open Ocean
Nyktericysta	*Deflandrea*	*Spiniferites*	*Impagidinium*
Homotryblium	*Wetzeliella*	*Hystrichosphaeridium*	*Nematosphaeropsis*
Eocladopyxis	*Glaphyrocysta*	*Cordosphaeridium*	*Pterodinium*
Polysphaeridium	*Areoligera*	*Hystrichokolpoma*	*Cannosphaeropsis*
Tuberculodinium	*Micrhystridium* (A)	*Cleistosphaeridium*	
Micrhystridium (A)	*Cleistosphaeridium*	*Operculodinium*	
Heteraulacacysta	*Dinogymnium*	*Phelodinium*	
Vesperopsis	*Heterosphaeridium*	*Cerodinium*	
	Phthanoperidinium		
	Cribroperidinium		

Figure 6.2 – Preferred paleoenvironments of common dinocyst taxa in the Labrador-Baffin Seaway. [from Nøhr-Hansen et al. in press]

7.0 Conclusion

New biostratigraphic ages have been determined for the Late Cretaceous to Early Paleogene strata at the South Coast section in Eclipse Trough. These ages were determined from palynological assemblages of 14 samples from five sections. Biostratigraphic evidence has demonstrated there is one hiatus. The entire Campanian is missing with Coniacian to Santonian strata unconformably overlain by Early Maastrichtian strata. Palynomorph assemblages have refined the Cretaceous-Paleogene (K/T) boundary, placing it in section 1 of the Pond Inlet formation [Figure 5.2 green]. The K/T boundary determined in this study is significantly higher in section 1 of the Pond Inlet formation than the K/T boundary determined by Sparkes (1989) and Waterfield (1989). The taxa across the K/T boundary show little variation, suggesting that dinocysts do not show evidence of a major extinction event at the end of the Cretaceous. This is consistent with the current notion that dinoflagellates were relatively unaffected by the major extinction event at the end of the Cretaceous. Danian and Selandian strata have been determined in sections 1 and 2 of the Pond Inlet formation [Figure 5.2].

The paleoenvironment of the South Coast section is neritic with distance from the coast increasing up section [Figure 6.1]. Palynomorph assemblages show that the Coniacian-Santonian sediments were deposited in inner neritic paleoenvironments. The Early Maastrichtian to Late Maastrichtian sediments were deposited in outer neritic paleoenvironments. The Late Maastrichtian to Danian sediments were deposited in outer neritic paleoenvironments. The Selandian sediments were deposited in outer/inner neritic paleoenvironments.

Biostratigraphic age refinements made in this thesis will provide direction for future sampling. More samples from the South Coast section would help refine the Campanian hiatus and may potentially refine the Cretaceous-Paleogene boundary. Refining the Campanian hiatus can be achieved by collecting/analysing samples from strata between sections G and K [Appendix A]. The Memorial group donated samples taken from sections between sections G and K, but processing of these samples yielded slides with poor palynomorph recovery. Further refining the Cretaceous-Paleogene boundary might be possible by collecting closely spaced samples from section 1 (between samples P5204-44 and P5201-53) [Figure 5.2].

The ages and paleoenvironments determined in this thesis help fill existing gaps in Bylot Island's biostratigraphic and paleoenvironmental records, helping to refine the current understanding of the Labrador-Baffin Seaway. The ages and paleoenvironments will also help in determining locations of future sampling on Bylot Island's South Coast.

References

Barss, M.S., & Williams G.L. (1974), Palynology and nannofossil processing techniques. Geological Survey of Canada. 73-26.

Evitt, W.R. (1961), Observations on the morphology of fossil dinoflagellates. Reprint from: Micropaleontology, Vol 7, no. 4, p.385-420

Falcon-Long, H., Fensome, R., Gensel, P., & Williams, G. (2014), Box 7. The Green Revolution. Chapter 7. Southern Sojourn: Canada 750 to 444 million years ago. In: Fensome, R. et al. (eds): Four billion years and counting: Canada's geological heritage. Halifax: Nimbus and Canadian Federation of Geological Sciences, p.126-129.

Fensome, R.A. (2015), Palynological analysis of two Labrador Shelf wells: Petro Canada et al. Rut H-11 and Eastcan et al. Karlsefni A-13. Geological Survey of Canada, In Press 7738, doi:10.4095/ 295616

Fensome, R.A., MacRae, R.A. & Williams, G.L. (2008), DINOFLAJ2, Version 1. American Association of Stratigraphic Palynologists, Data Series no. 1.

Fensome, R.A., Riding, J.B., & Taylor, F.J.R. (1996), Chapter 6. Dinoflagellates; in: Jansonius, J. & McGregor, D.C. (ed.), Palynology: Principles and application; American Association of Stratigraphic Palynologists Foundation, Vol 1, p.107-169.

Fensome, R.A., Taylor, F.J.R, Norris, G., Sarjeant, W.A.S., Wharton, D.I., & Williams, G.L. (1993), A classification of living and fossil dinoflagellates. Micropaleontology, Special Publication Number 7.

Fensome, R.A., Williams, G.L., MacRae, R.A. (2009), Late Cretaceous and Cenozoic fossil dinoflagellates and other palynomorphs from the Scotian Margin, offshore eastern Canada. Journal of Systematic Palaeontology, Vol 7, p.1-79. Doi:10.1017/S1477201908002538

Google earth V 7.1.2.2041. (March 7, 2016), Bylot Island, Nunavut, Canada. Eye alt 3417.99 km. Data SIO, NOAA, U.S. Navy, NGA, GEBCO. Image Landsat. Image U.S. Geological Survey. [Imagery Date: 12/13/2015]

Harland, R. (1973), Dinoflagellate cysts and acritarchs from the Bearpaw Formation (upper Campanian) of southern Alberta, Canada. Palaeontology, Vol 16, p.665–706.

Harrison, J.C., Brent, T.A., & Oakey, G.N. (2011), Baffin Fan and its inverted rift system of Arctic eastern Canada: stratigraphy, tectonics and petroleum resource potential. Geological Survey of Canada.

Ioannides, N.S. (1986), Dinoflagellate cysts from Upper Cretaceous–lower Tertiary sections, Bylot and Devon Islands, Arctic Archipelago. Geological Survey of Canada Bulletin 371, p.1–99.

Jackson, G.D., Davidson, A., & Morgan, W.C. (1975), Geology of the Pond Inlet map-area, Baffin Island, District of Franklin. Geological Survey of Canada. p.74-25.

Klassen, R.A. (1993), Quaternary Geology and Glacial History of Bylot Island, Northwest Territories. Geological Survey of Canada, Memoir 429.

Le Pichon, X., Hyndman, R.D., & Pautot, G. (1971), Geophysical study of the opening of the Labrador Sea. Journal of Geophysical Research, 76, 4724.

McGregor, E.D., Nielsen, S.B., Stephenson, R.A. (2014), Basin evolution in the Davis Strait area (West Greenland and conjugate East Baffin/Labrador passive margins) from thermostratigraphic and subsidence modelling of well data: Implications for tectonic evolution and petroleum systems. Bulletin of Canadian Petroleum Geology: Baffin Bay Special, Vol 62. no. 4, p.311.

Miall, A.D., Balkwill, H.R., & Hopkins Jr, W.S. (1980), Cretaceous and Tertiary Sediments of Eclipse Trough, Bylot Island Area, Arctic Canada, and Their Regional Setting. Geological Survey Paper 79-23.

Monger, J. et al. (2014), Chapter 9. Pangea Breaks Up and Mountains Rise: Canada 251 to 65.5 Million Years Ago. In: Fensome, R. et al. (eds): Four billion years and counting: Canada's geological heritage. Halifax: Nimbus and Canadian Federation of Geological Sciences, p.160–188.

Natural Resources Government of Canada (NRGC) (2016), GEM: Geo-Mapping for Energy and Minerals. Earth Sciences Federal Programs, Earth Science Resources. Retrieved from: http://www.nrcan.gc.ca/earth-sciences/resources/federal-programs/geomapping-energy-minerals/10904

Nøhr-Hansen, H. (1996), Upper Cretaceous dinoflagellate cyst stratigraphy, onshore West Greenland. Grønlands Geologiske Undersøgelse Bulletin 170, 104 pp.

Nøhr-Hansen, H. & Heilmann-Clausen, C. (2001), *Cerodinium kangiliense* sp. nov. and *Senegalinium iterlaaense* sp. nov. — two new, stratigraphic important Paleocene species from West Greenland and Denmark. Neues Jahrbuch für Paläontologie. Abhandlungen, Vol 219, p.153–170.

Nøhr-Hansen, H. (2000), Dinoflagellate cyst stratigraphy of the North Leif I-05 well, Hopedale Basin, Labrador Shelf, offshore eastern Canada. Danmarks og Grønlands Geologiske Undersøgelse Rapport 2004/109, 117pp, 2 Enclosures.

Nøhr-Hansen, H., Williams, G.L., & Fensome, R.A. (In Press), Biostratigraphic correlation of the western and eastern margins of the Labrador-Baffin Seaway and implications for the regional geology. Geologic Survey of Denmark and Greenland, Geologic Survey of Canada.

Oakey, G.N., & Chalmers, J.A. (2012), A new model for the Paleogene motion of Greenland relative to North America: Plate reconstructions of the Davis Strait and Nares Strait regions between Canada and Greenland, Journal of Geophysical Research, Res., 117, B10401, doi:10.1029/2011JB008942

Powell, A.J., Brinkhuis, H. & Bujak, J.P. (1996), Upper Paleocene–lower Eocene dinoflagellate cyst sequence biostratigraphy of southeast England. In: Knox, R.W.O.B. et al. (eds): Correlation of the early Paleogene in northwest Europe. Geological Society Special Publication (London) Vol 101, p.145–183.

Riding, J.B., Mantle, D.J., & Backhouse, J. (2010), A review of the chronostratigraphic ages of Middle Triassic to Late Jurassic dinoflagellate cyst biozones of the North West Shelf of Australia. Review of Palaeobotony and Palynology Vol. 162, p.543-575.

Sønderholm, M., Christiansen, F.G., Olsen, J.C., Planke, S., Bojesen-Koefoed, J.A., Dalhoff, F., Nielsen, T., Myklebust, R. & Nøhr-Hansen, H. (2003), Early rifting of the Labrador Sea and Baffin Bay: new evidence form seismic, well and sea-bed data. American Association of Petroleum Geologists International Conference and Exhibition, Barcelona, Spain. Programme with abstracts, A90.

Sparkes, K.E. (1989), Stratigraphy and terrestrial palynology of Late Cretaceous Eclipse Group strata, Bylot Island, Northwest Territories, Canada. Unpublished M.Sc. thesis, Memorial University of Newfoundland, St. Johns, Newfoundland and Labrador, 195 p.

Waterfield, J.J. (1989), Stratigraphy, sedimentology and palynology of Cretaceous and Tertiary strata, southwest Bylot Island, Northwest Territories, Canada. Unpublished M.Sc. thesis, Memorial University of Newfoundland, St. Johns, Newfoundland and Labrador, 260 p.

Williams, G.L. (2007), Palynological analysis of Chevron et al. South Labrador N-79, Hopedale Basin, Labrador Basin. Geological Survey of Canada Open File Report 5446, 26p. (1 sheet)

Williams, G.L., Brinkhuis, H., Pearce, M.A., Fensome, R.A., & Weegink, J.W. (2004), Southern Ocean and global dinoflagellate cyst events compared: index events for the Late Cretaceous–Neogene. In: Exon, N.F. et al. (eds) : Proceedings of the Ocean Drilling Program, Scientific Results 189, p.1–98.

Williams, G.L., Fensome, R.A., Miller, M.A., & Sarjeant, W.A.S. (2000), A glossary of the terminology applied to dinoflagellates, acritarchs and prasinophytes, with emphasis on fossils: third edition. AASP Contributions Series Number 37. American Association of Stratigraphic Palynologists Foundation.

Williams, G.L., Fensome, R.A., Brinkhuis, H., & Pross, J. (2009), The Paleobiology of Dinoflagellates. A text revised for the dinoflagellate short course in Urbino, July 2009.

Vernal, A.D., Henry, M., Bilodeau, G., Steinhauer, S., & Gibb, O. (2010), Micropaleontological preparation techniques and analyses. Department des Sciences de la Terre, UQAM.